Massive MIMO-Enabled Full-Duplex Cellular Networks

Arman Shojaeifard, *Member, IEEE*, Kai-Kit Wong, *Fellow, IEEE*, Marco Di Renzo, *Senior Member, IEEE*, Gan Zheng, *Senior Member, IEEE*, Khairi Ashour Hamdi, *Senior Member, IEEE*, Jie Tang, *Member, IEEE*

***Abstract*—We provide a theoretical framework for the study of massive multiple-input multiple-output (MIMO)-enabled full-duplex (FD) cellular networks in which the residual self-interference (SI) channels follow the Rician distribution and other channels are Rayleigh distributed. In order to facilitate bi-directional wireless functionality, we adopt (i) in the downlink (DL), a linear zero-forcing with self-interference-nulling (ZF-SIN) precoding scheme at the FD base stations (BSs), and (ii) in the uplink (UL), a self-interference-aware (SIA) fractional power control mechanism at the FD mobile terminals (MTs). Linear ZF receivers are further utilized for signal detection in the UL. The results indicate that the UL rate bottleneck in the FD baseline single-input single-output (SISO) system can be overcome via exploiting massive MIMO. On the other hand, the findings may be viewed as a reality-check, since we show that, under state-of-the-art system parameters, the spectral efficiency (SE) gain of FD massive MIMO over its half-duplex (HD) counterpart is largely limited by the cross-mode interference (CI) between the DL and the UL. In point of fact, the anticipated two-fold increase in SE is shown to be only achievable when the number of antennas tends to be infinitely large.**

***Index Terms*—Full-duplex, cellular network, massive MIMO, self-interference, cross-mode interference, uplink power control, Rician fading channel, stochastic geometry theory.**

I. Introduction

The fifth-generation mobile network (5G) is expected to roll out from 2018 onwards as a remedy for tackling the existing capacity crunch [3]. A key 5G technology is massive multiple-input multiple-output (MIMO), or large scale antenna system (LSAS), where the base stations (BSs) equipped with hundreds of antennas simultaneously communicate with multiple mobile terminals (MTs) [4]. Massive MIMO, via spatial-multiplexing and directing power intently, can greatly outperform the state-of-the-art cellular standards jointly in terms of spectral efficiency (SE) and energy efficiency (EE). Moreover, under increasingly scarce spectrum, the transceiving of information over the same radio-frequency (RF) resources, i.e. full-duplex (FD) mode [5], has become a topic of interest for 5G and beyond [6], [7]. In theory, FD technology can double the achievable sum-rate of half-duplex (HD) radios, where orthogonal RF partitioning is typically employed to avoid the over-powering self-interference (SI). In practice, however, the respective FD over HD SE gain predominantly depends on the SI cancellation capability.

Recently, there has been major breakthroughs in SI cancellation using any combination of (i) spatial/angular isolation and (ii) subtraction in digital/analog domains [8]. On the other hand, FD, beyond point-to-point, remains in its infancy. In particular, the introduction of cross-mode interference (CI) between the downlink (DL) and the uplink (UL), in addition to the SI, significantly increases the complexity for large scale FD cellular setups. Many relevant works have emerged recently, including FD for small-cell (SC) [9]–[11], relay (RL) [12]–[14], cloud radio access network (CRAN) [15], and heterogeneous cellular network (HCN) [16]–[18]. A general consensus from early results is that the FD over HD SE gain mostly arises in the DL and that the UL is the main performance bottleneck. For example, the authors in [19] have shown that bi-directional cellular systems with baseline single-input single-output (SISO), achieve double the DL rate at the cost of more than a thousand-fold reduction in the UL rate. A potential strategy for tackling this limitation is to exploit the large degrees of freedom (DoF) in massive MIMO for better resilience against SI and CI [20], [21].

A. Related Works

In [22], the authors considered a FD BS with large scale antenna array serving multiple HD single-antenna MTs, and proposed a linear extended zero-forcing (ZF) precoder to suppress SI at the receiving antennas, subject to perfect channel state information (CSI). The sum-rate in FD mode was almost doubled versus that in the HD case, and the optimal ratio of transmit over receive antennas was found to be approximately 3 [22]. The extension to a FD BS with large scale antenna array serving HD multi-antenna MTs using linear block diagonalization (BD) beamforming was provided in [23]. With asymptotically large antenna array size, the optimal ratio of transmit over receive antennas was shown

A. Shojaeifard and K.-K Wong are with the Communications and Information Systems Group, Department of Electronic and Electrical Engineering, University College London, London WC1E 7JE, United Kingdom. (e-mail: a.shojaeifard@ucl.ac.uk; kai-kit.wong@ucl.ac.uk).

M. Di Renzo is with the Laboratoire des Signaux et Systèmes, CNRS, CentraleSupélec, Univ Paris Sud, Université Paris-Saclay, 3 rue Joliot Curie, Plateau du Moulon, 91192, Gif-sur-Yvette, France. (e-mail: marco.direnzo@l2s.centralesupelec.fr).

G. Zheng is with the Wolfson School of Mechanical, Electrical, and Manufacturing Engineering, Loughborough University, Loughborough LE11 3TU, United Kingdom. (e-mail: g.zheng@lboro.ac.uk).

K. A. Hamdi is with the Microwave and Communication Systems Group, School of Electrical and Electronic Engineering, University of Manchester, Manchester M13 9PL, United Kingdom. (e-mail: k.hamdi@manchester.ac.uk).

J. Tang is with the School of Electronic and Information Engineering, South China University of Technology, Guangzhou, and with the State Key Laboratory of Integrated Services Networks, Xidian University, China. (e-mail: eejtang@scut.edu.cn).

This work was supported by the United Kingdom Engineering and Physical Sciences Research Council (EPSRC) under Grants EP/N008219/1 and EP/N007840/1, and by the National Natural Science Foundation of China under Grant 61601186.

Parts of this work were presented at the IEEE GLOBECOM 2016, Washington, D.C., United States [1], and at the IEEE ICC 2017, Paris, France [2].

to converge to the ratio of DL over UL streams. In [24], under a setup similar to that in [22], the FD sum-rates with different spatial isolation and SI subtraction methods were compared. On the other hand, non-linear transceiver design for maximizing the sum-rate in FD multi-user MIMO was studied in [25] and [26]. The works highlighted above have considered a single-cell network. Intuitively, the introduction of SI and CI has huge implications in a FD multi-cell multi-user MIMO paradigm necessitating rigorous investigation.

Several studies of FD multi-cell MIMO cellular networks have also been recently reported. In [27], the DL and UL ergodic sum-rates in a deterministic FD multi-cell multi-user MIMO setup were characterized using conjugate-beamforming (CB). In addition, the throughput performance in FD distributed MIMO systems with BS cooperation (i.e., FD network MIMO) was investigated in [28]. In particular, the authors utilized spatial interference-alignment (IA) for tackling the CI bottleneck, and characterized the FD over HD multiplexing gain in closed-form. Moreover, in [29], success probability expressions in cellular systems with FD relaying BSs under different beamforming and interference-cancellation strategies were characterized using stochastic geometry theory. On the other hand, the design and analysis of randomly-deployed FD cellular networks with directional antennas was provided in [30]. In particular, the authors derived analytical expressions for the DL and UL coverage probabilities under passive SI suppression and fixed power control.

B. Contributions

Motivated by the above, in this work, we provide a theoretical stochastic geometry-based framework for the study of FD massive MIMO cellular networks using the Poisson point process (PPP)-based abstraction model of BSs and MTs. We jointly consider the DL and UL of a FD multi-cell multi-user massive MIMO system where the BSs and MTs are transceiving over the same RF resources. We adopt the Rician distribution for the residual SI fading channels, thus capturing performance under generalized SI cancellation capability. All other fading channels are modeled using the Rayleigh distribution. In the DL, we devise a linear zero-forcing with self-interference-nulling (ZF-SIN) precoder to jointly suppress residual SI and multi-user interference. On the other hand, we propose a self-interference-aware (SIA) fractional power control mechanism at the FD MTs to keep SI below a certain threshold. We derive the distributions, and in certain cases moments of the proposed UL transmit power mechanism. Moreover, in the UL, for signal detection at the FD massive MIMO BSs, linear ZF receivers are utilized for suppressing multi-user interference.

The signals distributions are derived under the linear processes described above. We characterize the DL and UL SEs using a moment-generating-function (m.g.f.)-based approach and derive the signals conditional statistics in closed-form. The proposed framework can be readily used to calculate the SEs via three-fold integrals, versus (i) the manifold integrals involved in the direct capacity evaluation approach, and (ii) the highly resource-intensive Monte-Carlo (MC) simulations [31]. We further reduce the computational complexity in certain special cases. In particular, we adopt the proposed framework to study the FD versus HD cellular network performance. With baseline SISO, we derive a tight bounded closed-form function of the FD over HD SE gain and show its optimal point occurs in the ratio of the BS and MT transmit powers being equal to one. With massive MIMO, we derive single-integral expressions for the FD and HD SEs and hence utilize multivariate non-linear curve fitting to develop a closed-form approximation of the corresponding FD over HD SE gain as a function of the number of antennas and users.

The validity of the proposed theoretical framework is confirmed using MC simulations. Our findings highlight that the key characteristics of massive MIMO, in terms of high transmit/receive array gain and lower BS/MT transmit power, allow for achieving significant performance gains over other FD multi-cell setups. On the other hand, the SE gain of FD over HD massive MIMO cellular network, under state-of-the-art system parameters, is shown to be predominantly limited by the CI between the DL and the UL. In point of fact, the corresponding sum-rate gain is shown to increase only logarithmically in the antenna array size, with the anticipated two-fold increase in SE only achieved as the number of antennas tends to be infinitely large.

C. Organization

The remainder of this paper is organized as follows. The massive MIMO-enabled FD cellular network is described in Section II. The proposed UL power control mechanism is introduced in Section III. The SE analysis is provided in Section IV, followed by a comparison of FD over HD SE gain in Section V. Numerical results are provided in Section VI, and finally, conclusions are drawn in Section VII.

D. Notation

We use the following notation in this work. $\boldsymbol{X}$ is a matrix with (i,j)-th entry $\{\boldsymbol{X}\}_{i,j}$; $\boldsymbol{x}$ is a vector with k-th element $\{\boldsymbol{x}\}_k$; T, $\dagger$, and $+$ are the transpose, Hermitian, and pseudo-inverse operations; $\mathbb{E}_x\{.\}$ is the expectation; $\mathcal{F}_x(.)$ is the cumulative density function (c.d.f.); $\mathcal{P}_x(.)$ is the probability density function (p.d.f.); $\mathscr{P}(x)$ is the probability; $\mathcal{M}_x(.)$ is the m.g.f.; $|x|$ is the modulus; $\|\boldsymbol{x}\|$ and $\|\boldsymbol{X}\|$ are the Euclidean and Frobenius norms; $\mathbf{I}_{(.)}$ is the identity matrix; Null(.) is a nullspace; $\mathcal{H}(.)$ is the Heaviside step function; $\delta(.)$ is the Delta function; $\mathcal{CN}(\mu,\nu^2)$ is the complex Gaussian distribution with mean μ and variance ν^2; $\Gamma(.)$ and $\Gamma(.,.)$ are the Gamma and incomplete (upper) Gamma functions; $\Gamma(\kappa,\theta)$ is the Gamma distribution with shape parameter κ and scale parameter θ; $\mathcal{L}_n(.)$ is the Laguerre polynomial; Ei(.), $\mathscr{S}(.)$, and $\mathscr{C}(.)$ are the exponential, Sine, and Cosine integral functions; erfi(.) is the imaginary error function; $Q_m(.,.)$ is the Marcum Q-function; ${}_2F_1(.,.;.;.)$, ${}_2\tilde{F}_1(.,.;.;.)$, ${}_0F_1(;.;.)$, ${}_0\tilde{F}_1(;.;.)$, ${}_pF_q(.;.;.)$, ${}_p\tilde{F}_q(.;.;.)$ are the Gauss, Regularized Gauss, confluent, Regularized confluent, generalized, and Regularized generalized hypergeometric functions; and $\mathcal{G}_{p,q}^{m,n}(.\,|\,(.))$ is the Meijer-G function, respectively.

This article has been accepted for publication in a future issue of this journal, but has not been fully edited. Content may change prior to final publication. Citation information: DOI 10.1109/TCOMM.2017.2731768, IEEE Transactions on Communications

II. System Description

A. Network Topology

In this work, we consider a FD cellular setup with BSs and MTs respectively deployed on the two-dimensional Euclidean space according to independent stationary PPPs $\Phi^{(d)}$ and $\Phi^{(u)}$ with spatial densities $\lambda^{(d)}$ and $\lambda^{(u)}$. Let l and k denote the locations of the l-th BS and the k-th MT, respectively. Their respective Euclidean distance is therefore $d_{l,k} = \|l-k\|$. The BSs are assumed to be equipped with N_t transmit and N_r receive antennas ($N_t + N_r$ RF chains in total), respectively. The MTs are in turn assumed to be equipped with single transmit/receive antennas (two RF chains in total). Each FD BS, using linear beamforming, is considered to simultaneously serve $\mathcal{U}$ FD MTs in the DL and UL per resource block [32]. We assume the condition $\mathcal{U} \leq \min(N_t, N_r)$ holds, thus, scheduling is not required here.

By invoking the Slivnyak's theorem [33], the DL analysis is carried out for an arbitrary MT o assumed to be located at the center. Here, we consider a cellular association strategy where the reference MT is served by a massive MIMO BS b which provides the greatest received signal power. For homogeneous cellular deployments, this is equivalent to the cellular association strategy based on the closest transmitter-receiver distance, i.e., $b = \arg\max \left(d_{l,o}^{-\beta}\right),\ \forall l \in \Phi^{(d)}$ [34]. The UL analysis, on the other hand, is carried out for the reference MT o signal at its serving massive MIMO BS b. The corresponding transceiver distance p.d.f. is given by $\mathcal{P}_{d_{b,o}}(r) = 2\pi\lambda^{(d)} r \exp\left(-\pi\lambda^{(d)} r^2\right)$. Note that the alternative decoupling approach for cellular association [35] results in the loss of channel reciprocity in massive MIMO systems.

It is important to note that the set of scheduled MTs is *strictly not* an independent process as a result of the inherent spatial dependencies arising from (i) the cellular association strategy, and (ii) the constraint of each BS serving multiple MTs per resource block. For the sake of mathematical tractability, in the same spirit as in [36], we invoke the following assumption.

Assumption 1. *The set of scheduled MTs, conditioned on the spatial constraints imposed by the cellular association strategy and the number of MTs being served by each BS per resource block, is modeled as an independent stationary PPP with density $\lambda^{(u)}$.*

B. Channel Model

Let $\boldsymbol{g}_{l,k} \in \mathcal{C}^{1\times N_t}$, $\boldsymbol{G}_{l,j} \in \mathcal{C}^{N_r\times N_t}$, and $\boldsymbol{G}_{l,l} \in \mathcal{C}^{N_r\times N_t}$ denote the channel from the l-BS to the k-th MT, the channel from the l-th BS to the j-th BS, and the residual SI channel at the l-th BS, respectively. Moreover, $\boldsymbol{h}_{k,l} \in \mathcal{C}^{N_r\times 1}$, $h_{k,i}$, and $h_{k,k}$ are respectively the channel from the k-th MT to the l-th BS, the channel from the k-th MT to the i-th MT, and the residual SI channel at the k-th MT. The residual SI (for brevity, hereafter, refered to as SI) channels are subject to Rician fading with independent and identically-distributed (i.i.d.) elements drawn from $\mathcal{CN}(\mu, \upsilon^2)$. All other channels are modeled using Rayleigh fading with i.i.d. elements drawn from $\mathcal{CN}(0,1)$. Here, we use the unbounded distance-dependent path-loss model with exponent β (> 2). Note that CSI in time-division duplex (TDD)-based massive MIMO systems can be acquired based on channel reciprocity through UL training. In this work, we assume sophisticated channel estimation algorithms with sufficient training information are used to obtain perfect CSI [37]. The reader is referred to [38] for the impact of imperfect CSI on the performance of multi-cell multi-user massive MIMO systems.

C. Beamforming Design

Next, we discuss the linear precoding and decoding strategies for the massive MIMO-enabled FD cellular network under consideration.

Let $\boldsymbol{G}_l = [\boldsymbol{g}_{l,k}^T]_{1\leq k\leq \mathcal{U}}^T \in \mathcal{C}^{\mathcal{U}\times N_t}$ denote the combined DL channels from the l-th BS to its $\mathcal{U}$ MTs. We use $\boldsymbol{s}_l = [s_{l,k}]_{1\leq k\leq \mathcal{U}}^T \in \mathcal{C}^{\mathcal{U}\times 1}$, $\mathbb{E}\left\{|s_{l,k}|^2\right\} = 1$, to denote the DL complex symbol vector from the l-th BS to its $\mathcal{U}$ MTs. Here, we consider the case where each BS equally allocates its total transmit power $p^{(d)}$ among its $\mathcal{U}$ MTs. The normalized precoding matrix at the l-th BS is $\boldsymbol{V}_l = [\boldsymbol{v}_{l,k}]_{1\leq k\leq \mathcal{U}} \in \mathcal{C}^{N_t\times \mathcal{U}}$, $\mathbb{E}\left\{\|\boldsymbol{v}_{l.k}\|^2\right\} = 1$. Hence, the DL received signal is given by (1), as shown at the top of the next page, where $\Phi_l^{(u)}$ ($\subset \Phi^{(u)}$) is the set of scheduled MTs in the cell of BS l, $p_{k,l}^{(u)}$ is the k-th scheduled MT transmit power for sending $s_{k,l}$ to BS l, and η_o is the complex additive white Gaussian noise (AWGN) with mean zero and variance σ_d^2, respectively.

Next, let $\boldsymbol{H}_l = [\boldsymbol{h}_{k,l}]_{1\leq k\leq \mathcal{U}} \in \mathcal{C}^{N_r\times \mathcal{U}}$ represent the compound UL channel matrix at the l-BS with respect to its $\mathcal{U}$ scheduled MTs. The normalized decoding matrix at the l-th BS is denoted using $\boldsymbol{W}_l = [\boldsymbol{w}_{k,l}^T]_{1\leq k\leq \mathcal{U}}^T \in \mathcal{C}^{\mathcal{U}\times N_r}$, $\mathbb{E}\left\{\|\boldsymbol{w}_{k,l}\|^2\right\} = 1$. The corresponding post-processing UL signal is given by (2), as shown at the top of the next page, where $\boldsymbol{\eta}_b \in \mathcal{C}^{N_r\times 1}$ is the AWGN vector with mean zero and covariance matrix $\sigma_u^2 \mathbf{I}_{N_r}$.

Proposition 1. *In the DL, we adopt a linear ZF-SIN precoder where the transmit antenna array (conditioned on $N_t \geq N_r + \mathcal{U}$) is utilized to jointly suppress SI and multi-user interference at the receiving antennas. This is achieved at the BS l by setting the columns of $\boldsymbol{V}_l$ equal to the normalized columns of $\hat{\boldsymbol{G}}_l^+ = \hat{\boldsymbol{G}}_l^\dagger(\hat{\boldsymbol{G}}_l\hat{\boldsymbol{G}}_l^\dagger)^{-1} = [\hat{\boldsymbol{g}}_{l,k}]_{1\leq k\leq \mathcal{U}} \in \mathcal{C}^{N_t\times \mathcal{U}}$ where $\hat{\boldsymbol{G}}_l = \boldsymbol{G}_l(\boldsymbol{I}_{N_t} - \boldsymbol{G}_{l,l}^\dagger(\boldsymbol{G}_{l,l}\boldsymbol{G}_{l,l}^\dagger)^{-1}\boldsymbol{G}_{l,l})$.*

Proof: See Appendix A.

Note that the proposed null-steering precoder differs from the extended ZF scheme in [22] where 'all-zero' streams are sent for the purpose of suppressing SI, i.e., in [22] the (normalized) transmit signal vector $\mathbf{V}_l \cdot \begin{bmatrix} \boldsymbol{s}_l \\ \mathbf{0}_{N_r\times 1} \end{bmatrix}$ with $\mathbf{V}_l \in \mathcal{C}^{N_t\times(\mathcal{U}+N_r)}$ is set equal to the normalized columns of $\hat{\boldsymbol{G}}_l^+ = \hat{\boldsymbol{G}}_l^\dagger(\hat{\boldsymbol{G}}_l\hat{\boldsymbol{G}}_l^\dagger)^{-1} = [\hat{\boldsymbol{g}}_{l,k}]_{1\leq j\leq \mathcal{U}+N_r} \in \mathcal{C}^{N_t\times(\mathcal{U}+N_r)}$ where $\hat{\boldsymbol{G}}_l = \begin{bmatrix} \boldsymbol{G}_l \\ \mathbf{G}_{l,l} \end{bmatrix}$.

Proposition 2. *In the UL, a linear ZF decoder, eliminating multi-user interference, is employed with the normalized rows of $\boldsymbol{H}_l^+ = (\boldsymbol{H}_l^\dagger\boldsymbol{H}_l)^{-1}\boldsymbol{H}_l^\dagger = [\hat{\boldsymbol{h}}_{k,l}^T]_{1\leq k\leq \mathcal{U}}^T \in \mathcal{C}^{\mathcal{U}\times N_r}$ set as the row vectors of $\boldsymbol{W}_l$, at the BS l.*

In the subsequent parts of this section, we characterize the DL and UL signal-to-interference-plus-noise ratios (SINRs).

This article has been accepted for publication in a future issue of this journal, but has not been fully edited. Content may change prior to final publication. Citation information: DOI 10.1109/TCOMM.2017.2731768, IEEE Transactions on Communications

$$y_d = \underbrace{\sqrt{\frac{p^{(d)}}{\mathcal{U}}} d_{b,o}^{-\frac{\beta}{2}} \boldsymbol{g}_{b,o} \boldsymbol{v}_{b,o} s_{b,o}}_{d \text{ (intended signal)}} + \underbrace{\sqrt{\frac{p^{(d)}}{\mathcal{U}}} d_{b,o}^{-\frac{\beta}{2}} \boldsymbol{g}_{b,o} \sum_{k \in \Phi_b^{(u)} \setminus \{o\}} \boldsymbol{v}_{b,k} s_{b,k}}_{dd \text{ (multi-user interference)}} + \underbrace{\sqrt{\frac{p^{(d)}}{\mathcal{U}}} \sum_{l \in \Phi^{(d)} \setminus \{b\}} d_{l,o}^{-\frac{\beta}{2}} \boldsymbol{g}_{l,o} \boldsymbol{V}_l \boldsymbol{s}_l}_{d,d \text{ (inter-cell interference)}}$$
$$+ \underbrace{\sum_{k \in \Phi_l^{(u)}, l \in \Phi^{(d)} \setminus \{o,b\}} \sqrt{p_{k,l}^{(u)}} d_{k,o}^{-\frac{\beta}{2}} h_{k,o} s_{k,l}}_{u,d \text{ (cross-mode interference)}} + \underbrace{\sqrt{p_{o,b}^{(u)}} h_{o,o} s_{o,b}}_{si,d \text{ (self-interference)}} + \underbrace{\eta_o}_{\text{noise}} \tag{1}$$

$$y_u = \underbrace{\sqrt{p_{o,b}^{(u)}} d_{o,b}^{-\frac{\beta}{2}} \boldsymbol{w}_{o,b}^T \boldsymbol{h}_{o,b} s_{o,b}}_{u \text{ (intended signal)}} + \underbrace{\sum_{k \in \Phi_b^{(u)} \setminus \{o\}} \sqrt{p_{k,b}^{(u)}} d_{k,b}^{-\frac{\beta}{2}} \boldsymbol{w}_{o,b}^T \boldsymbol{h}_{k,b} s_{k,b}}_{uu \text{ (multi-user interference)}} + \underbrace{\sum_{k \in \Phi_l^{(u)}, l \in \Phi^{(d)} \setminus \{b\}} \sqrt{p_{k,l}^{(u)}} d_{k,b}^{-\frac{\beta}{2}} \boldsymbol{w}_{o,b}^T \boldsymbol{h}_{k,b} s_{k,l}}_{u,u \text{ (inter-cell interference)}}$$
$$+ \underbrace{\sqrt{\frac{p^{(d)}}{\mathcal{U}}} \sum_{l \in \Phi^{(d)} \setminus \{b\}} d_{l,b}^{-\frac{\beta}{2}} \boldsymbol{w}_{o,b}^T \boldsymbol{G}_{l,b} \boldsymbol{V}_l \boldsymbol{s}_l}_{d,u \text{ (cross-mode interference)}} + \underbrace{\sqrt{\frac{p^{(d)}}{\mathcal{U}}} \boldsymbol{w}_{o,b}^T \boldsymbol{G}_{b,b} \boldsymbol{V}_b \boldsymbol{s}_b}_{si,u \text{ (self-interference)}} + \underbrace{\boldsymbol{w}_{o,b}^T \boldsymbol{\eta}_b}_{\text{noise}} \tag{2}$$

D. Downlink SINR

The DL received SINR at the reference MT is given by

$$\gamma_d = \frac{\mathcal{X}_d}{\mathcal{I}_{d,d} + \mathcal{I}_{u,d} + \mathcal{I}_{si,d} + \sigma_d^2} \tag{3}$$

where $\mathcal{X}_d = \frac{p^{(d)}}{\mathcal{U}} d_{b,o}^{-\beta} G_{b,o}$, $\mathcal{I}_{d,d} = \frac{p^{(d)}}{\mathcal{U}} \sum_{l \in \Phi^{(d)} \setminus \{b\}} d_{l,o}^{-\beta} G_{l,o}$, $\mathcal{I}_{u,d} = \sum_{k \in \Phi_l^{(u)}, l \in \Phi^{(d)} \setminus \{o,b\}} p_{k,l}^{(u)} d_{k,o}^{-\beta} H_{k,o}$, $\mathcal{I}_{si,d} = p_{o,b}^{(u)} H_{o,o}$, $G_{b,o} \triangleq |\boldsymbol{g}_{b,o} \boldsymbol{v}_{b,o}|^2$, $G_{l,o} \triangleq \|\boldsymbol{g}_{l,o} \boldsymbol{V}_l\|^2$, $H_{k,o} \triangleq |h_{k,o}|^2$, and $H_{o,o} \triangleq |h_{o,o}|^2$. The ZF-SIN precoding vector $\boldsymbol{v}_{b,o} = \frac{\hat{\boldsymbol{g}}_{b,o}}{\|\hat{\boldsymbol{g}}_{b,o}\|}$ is selected in the direction of the projection of $\boldsymbol{g}_{b,0}$ on $\text{Null}([\boldsymbol{g}_{b,k}]_{1 \le k \le \mathcal{U}, k \ne 0}, \boldsymbol{G}_{b,b})$. The nullspace spanned by the SI and multi-user interference is $D_d \triangleq N_t - N_r - \mathcal{U} + 1$ dimensional. For analytical tractability, we assume that the outer-cell precoding matrices have independent column vectors [36], [39]. As a result, the channel power gain from each interfering BS in the DL is interpreted as the aggregation of multiple separate beams from the projection of the cross-link channel vector $\boldsymbol{g}_{l,o}$ onto the one-dimensional precoding vectors $\boldsymbol{v}_{l,k}$. The scheduled MTs, on the other hand, transmit using single-antennas (in all directions).

Assumption 2. *The channel power gains at the reference MT o, from the intended BS b, interfering BS l, and scheduled MT k, are respectively $G_{b,o} \sim \Gamma(D_d, 1)$, $G_{l,o} \approx \Gamma(\mathcal{U}, 1)$, and $H_{k,o} \sim \Gamma(1,1)$. Note that the p.d.f. and m.g.f. expressions of a Gamma-distributed random variable $G_{(.)}$ with shape parameter κ and scale parameter θ can be respectively expressed as*

$$\mathcal{P}_{G_{(.)}}(g) = \frac{g^{\kappa-1}}{\theta^\kappa \Gamma(\kappa)} \exp\left(-\frac{g}{\theta}\right) \tag{4}$$

and

$$\mathcal{M}_{G_{(.)}}(z) = \frac{1}{(1+\theta z)^\kappa}. \tag{5}$$

Remark 1. *Utilizing the linear ZF-SIN precoder for spatially suppressing SI at the BS side results in a loss of N_r (number of receive antennas) DoF in the DL antenna array gain.*

The Rayleigh fading model applies to cases without line-of-sight (LOS), e.g., with afar transceiver distances. In FD setups, however, the nodes transmit and receive antennas are co-located. Hence, the Rician fading model, which takes into account the different LOS and scattered paths, can be invoked to capture performance under generalized SI cancellation capability [8].

Assumption 3. *The SI channel power gain at the reference MT o is a non-central Chi-squared random variable with Rician factor K and fading attenuation Ω, such that $\mu \triangleq \sqrt{\frac{K\Omega}{K+1}}$ and $\nu \triangleq \sqrt{\frac{\Omega}{K+1}}$. The corresponding p.d.f. and m.g.f. are respectively given by*

$$\mathcal{P}_{H_{o,o}}(h) = \frac{1+K}{\Omega} \exp\left(-\left(K + \frac{(1+K)h}{\Omega}\right)\right) \times I_0\left(2\sqrt{\frac{K(1+K)h}{\Omega}}\right) \tag{6}$$

and

$$\mathcal{M}_{H_{o,o}}(z) = \frac{1+K}{1+K+z\Omega} \exp\left(-\frac{zK\Omega}{1+K+z\Omega}\right). \tag{7}$$

It should be noted that the modified Bessel function of the first kind can be expressed through hypergeometric functions, e.g., here, $I_0(\chi) = {}_0\tilde{F}_1\left(;1;\left(\frac{\chi}{2}\right)^2\right)$.

Remark 2. *The SI channel power gain at the reference MT o can be approximated using Gamma moment matching as $H_{o,o} \approx \Gamma(\kappa, \theta)$, where $\kappa \triangleq \frac{\left(\mu^2+\nu^2\right)^2}{(2\mu^2+\nu^2)\nu^2}$ and $\theta \triangleq \frac{\left(2\mu^2+\nu^2\right)\nu^2}{\mu^2+\nu^2}$ [40].*

This article has been accepted for publication in a future issue of this journal, but has not been fully edited. Content may change prior to final publication. Citation information: DOI 10.1109/TCOMM.2017.2731768, IEEE Transactions on Communications

E. Uplink SINR

Next, we express the UL received SINR from the reference MT at its serving BS as

$$\gamma_u = \frac{\mathcal{X}_u}{\mathcal{I}_{u,u} + \mathcal{I}_{d,u} + \sigma_u^2} \tag{8}$$

where $\mathcal{X}_u = p_{o,b}^{(u)} d_{o,b}^{-\beta} H_{o,b}$, $\mathcal{I}_{u,u} = \sum_{k\in\Phi_l^{(u)}, l\in\Phi^{(d)}\setminus\{b\}} p_{k,l}^{(u)} d_{k,b}^{-\beta} H_{k,b}$, $\mathcal{I}_{d,u} = \frac{p^{(d)}}{\mathcal{U}} \sum_{l\in\Phi^{(d)}\setminus\{b\}} d_{l,b}^{-\beta} G_{l,b}$, $H_{o,b} \triangleq |\boldsymbol{w}_{o,b}^T \boldsymbol{h}_{o,b}|^2$, $H_{k,b} \triangleq |\boldsymbol{w}_{o,b}^T \boldsymbol{h}_{k,b}|^2$, and $G_{l,b} \triangleq \|\boldsymbol{w}_{o,b}^T \boldsymbol{G}_{l,b} \boldsymbol{V}_l\|^2$. Note $\|\hat{\boldsymbol{h}}_{o,b}^T\|^{-2} = \{(\boldsymbol{H}_b^\dagger \boldsymbol{H}_b)^{-1}\}_{o,o} \sim \text{Erlang}(D_u, 1)$ where $D_u \triangleq N_r - \mathcal{U} + 1$. In turn, $\boldsymbol{W}_b$ is selected independently from $\boldsymbol{h}_{k,b}$ and $\boldsymbol{G}_{l,b}$. We recall the assumption that $\boldsymbol{V}_l$ has independent column vectors.

Assumption 4. *The channel power gains at the reference BS b, from the intended MT o, interfering MT k, and interfering BS l are respectively modeled using $H_{o,b} \sim \Gamma(D_u, 1)$, $H_{k,b} \sim \Gamma(1,1)$, and $G_{l,b} \approx \Gamma(\mathcal{U}, 1)$.*

It is important to note that it is certainly feasible to apply other linear precoding schemes such as CB in FD massive MIMO systems [27]. In such cases, the SI channel power gain, e.g., at the reference BS b, $G_{b,b} \triangleq \|\boldsymbol{w}_{o,b}^T \boldsymbol{G}_{b,b} \boldsymbol{V}_b\|^2$, needs to be characterized. In [40], the distribution of the SI with arbitrary linear beamforming design over FD multi-user MIMO Rician fading channels was approximated using Gamma moment matching. In particular, for FD multi-user massive MIMO systems, we obtain the following result.

Corollary 1. *With arbitrary linear precoders in the DL (such as CB and ZF), the SI channel power gain at the reference massive MIMO BS b can be approximated using Gamma moment matching as $G_{b,b} \approx \Gamma(\kappa, \theta)$, where $\kappa = \frac{\mathcal{U}\left(\mu^2+\nu^2\right)^2}{(\mathcal{U}+2)\mu^4+2\mu^2\nu^2+\nu^4}$ and $\theta = \frac{(\mathcal{U}+2)\mu^4+2\mu^2\nu^2+\nu^4}{\mu^2+\nu^2}$ [40].*

In the case of imperfect knowledge of SI channel, one has to account for the impact of estimation error. For example, let $\hat{\boldsymbol{G}}_{b,b} \in \mathcal{C}^{N_r \times N_t}$ denote the minimum mean-square error (MMSE) estimate of $\boldsymbol{G}_{b,b}$. Consider the estimation error given by $\boldsymbol{\xi}_{b,b} \triangleq \hat{\boldsymbol{G}}_{b,b} - \boldsymbol{G}_{b,b}$ with elements drawn independently from $\mathcal{CN}(\varpi, \varsigma^2)$. Hence, we can characterize the corresponding average SI as in the following result.

Corollary 2. *With the MMSE estimation process above, under arbitrary linear beamforming design, the average SI channel power gain at the reference massive MIMO BS b in the UL is given by $\mathbb{E}\{\|\boldsymbol{w}_{o,b}^T \hat{\boldsymbol{G}}_{b,b} \boldsymbol{V}_b\|^2\} = \mathbb{E}\left\{\sum_{k=1}^{\mathcal{U}} |\boldsymbol{w}_{o,b}^T \boldsymbol{\xi}_{b,b} \boldsymbol{v}_{b,k}|^2\right\} = \mathcal{U}(\varpi^2 + \varsigma^2)$ [40].*

III. Self-Interference-Aware Power Control

In long-term-evolution (LTE) standards, UL fractional power control is defined to account for the path-loss effect [41]. Recently, interference-aware fractional power control has been proposed to ensure that the power adjustment intended for path-loss compensation does not cause undesired interference to neighboring nodes [42]. Intuitively, power control has perhaps an even more essential role to play in FD cellular setups. This topic remains somewhat unexplored however.

In this work, we propose an LTE-compliant SIA fractional power control mechanism where the MTs adjust their transmit power based on the distance-dependent path-loss, SI, and maximum available transmit power. The motivation behind this is in line with the notion that the MTs with limited number of antennas rely on digital/analog domain interference cancellation strategies, and hence may experience severe SI and CI affecting the DL operation.

Specifically, in this work, an arbitrary scheduled MT k transmits to its serving BS l using

$$p_{k,l}^{(u)} = \min\left(p_0 d_{k,l}^{\psi\beta}, I_{\text{SI}} H_{k,k}^{-1}, p^{(u)}\right) \tag{9}$$

where p_0, ψ $(\in (0,1])$, I_{SI}, and $p^{(u)}$ are respectively the normalized power density, compensation factor, tolerable SI level, and maximum transmit power at the MT [36]. The value of I_{SI} can be set as the difference in the noise floor power from the gain of the MT SI cancellation capability. The distribution of the transmit power in this setup can be developed.

Lemma 1. *The c.d.f. and p.d.f. of the transmit power of a typical MT under the SIA fractional power control mechanism, $p_{k,l}^{(u)} = \min\left(p_0 d_{k,l}^{\psi\beta}, I_{SI} H_{k,k}^{-1}, p^{(u)}\right)$, are respectively given by (10) and (11), as shown at the top of the next page, where $\Xi_{\text{I}}(p) = \pi\lambda^{(d)}\left(\frac{p}{p_0}\right)^{\frac{2}{\psi\beta}}$ and $\Xi_{\text{II}}(p) = \frac{I_{SI}}{p\Omega}$.*

Proof: See Appendix B.

Remark 3. *The proposed LTE-compliant SIA fractional power control mechanism can be viewed as a generalization of the existing approaches for UL power control including total (without I_{SI}) and truncated (without I_{SI} and $p^{(u)}$) fractional power control schemes.*

The computation of SE can be greatly simplified with a non-direct methodology requiring only the moments of the signals involved [43]. On the other hand, the p.d.f. expression in (11), is a highly non-linear piecewise function. Hence, the exact moments of the proposed SIA fractional power control mechanism required for the calculation of SE cannot be derived in closed-form. Next, we develop results for the moments of the SIA power control in certain special cases where the corresponding p.d.f. has a more tractable form. It should be noted that a Meijer-G function can be readily calculated using common software for numerical computation. A Meijer-G function can also be expressed in terms of a hypergeometric function based on the results from [44].

Corollary 3. *The p.d.f. of the transmit power of a typical MT under the SIA fractional power control mechanism can be simplified in certain special cases.*

For $K = 0$ (Rayleigh SI channel), $p_0 \to +\infty$ (no path-loss compensation), and $I_{SI} \to +\infty$ (no constraint on the SI), we respectively obtain (12), (13), and (14), as shown at the top of the next page.

Lemma 2. *The $\flat$-th positive moment of the transmit power of a typical MT under the SIA fractional power control mechanism admits a closed-form expression in certain special cases. Let $\hat{\Xi}_{\text{I}} = \frac{\pi\lambda^{(d)}}{p_0^{\frac{2}{\beta\psi}}}$ and $\hat{\Xi}_{\text{II}} = \frac{I_{SI}}{\Omega}$.*

This article has been accepted for publication in a future issue of this journal, but has not been fully edited. Content may change prior to final publication. Citation information: DOI 10.1109/TCOMM.2017.2731768, IEEE Transactions on Communications

$$\mathcal{F}_{p_{k,l}^{(u)}}(p)=\left(1-\exp\left(-\Xi_{\mathrm{I}}(p)\right)\left(1-Q_1\left(\sqrt{2K},\sqrt{2(1+K)\Xi_{\mathrm{II}}(p)}\right)\right)\right)\left(1-\mathcal{H}\left(p-p^{(u)}\right)\right)+\mathcal{H}\left(p-p^{(u)}\right) \tag{10}$$

$$\mathcal{P}_{p_{k,l}^{(u)}}(p)=\begin{cases}\exp\left(-\Xi_{\mathrm{I}}\left(p^{(u)}\right)\right)\left(1-Q_1\left(\sqrt{2K},\sqrt{2(1+K)\Xi_{\mathrm{II}}\left(p^{(u)}\right)}\right)\right)\delta\left(p-p^{(u)}\right) & p\geq p^{(u)}\\ \dfrac{\exp\left(-\Xi_{\mathrm{I}}(p)\right)}{p}\left[\dfrac{2\Xi_{\mathrm{I}}(p)}{\psi\beta}\left(1-Q_1\left(\sqrt{2K},\sqrt{2(1+K)\Xi_{\mathrm{II}}(p)}\right)\right)+(1+K)\Xi_{\mathrm{II}}(p)\right. & \\ \left.\times\exp\left(-\left(K+(1+K)\Xi_{\mathrm{II}}(p)\right)\right){}_0\tilde{F}_1\left(;1;K(1+K)\Xi_{\mathrm{II}}(p)\right)\right] & p<p^{(u)}\end{cases} \tag{11}$$

$$\mathcal{P}_{p_{k,l}^{(u)}}(p)=\begin{cases}\exp\left(-\Xi_{\mathrm{I}}\left(p^{(u)}\right)\right)\left(1-\exp\left(-\Xi_{\mathrm{II}}\left(p^{(u)}\right)\right)\right)\delta\left(p-p^{(u)}\right) & p\geq p^{(u)}\\ \dfrac{\exp\left(-\Xi_{\mathrm{I}}(p)\right)}{p}\left(\dfrac{2\Xi_{\mathrm{I}}(p)}{\psi\beta}\left(1-\exp\left(-\Xi_{\mathrm{II}}(p)\right)\right)+\Xi_{\mathrm{II}}(p)\exp\left(-\Xi_{\mathrm{II}}(p)\right)\right) & p<p^{(u)}\end{cases} \tag{12}$$

$$\mathcal{P}_{p_{k,l}^{(u)}}(p)=\begin{cases}\left(1-Q_1\left(\sqrt{2K},\sqrt{2(1+K)\Xi_{\mathrm{II}}\left(p^{(u)}\right)}\right)\right)\delta\left(p-p^{(u)}\right) & p\geq p^{(u)}\\ (1+K)\Xi_{\mathrm{II}}\left(p^2\right)\exp\left(-\left(K+(1+K)\Xi_{\mathrm{II}}(p)\right)\right){}_0\tilde{F}_1\left(;1;K(1+K)\Xi_{\mathrm{II}}(p)\right) & p<p^{(u)}\end{cases} \tag{13}$$

$$\mathcal{P}_{p_{k,l}^{(u)}}(p)=\begin{cases}\left(1-\exp\left(-\Xi_{\mathrm{I}}\left(p^{(u)}\right)\right)\right)\delta\left(p-p^{(u)}\right) & p\geq p^{(u)}\\ \dfrac{2\Xi_{\mathrm{I}}(p)}{\psi\beta p}\exp\left(-\Xi_{\mathrm{I}}(p)\right) & p<p^{(u)}\end{cases} \tag{14}$$

$$\mathbb{E}\left\{{p_{k,l}^{(u)}}^{\flat}\right\}=\frac{\hat{\Xi}_{\mathrm{II}}^{\flat}}{\sqrt{\pi}}\left(\mathcal{G}_{0,3}^{3,0}\left(-\flat+1,0,\tfrac{1}{2}\,\middle|\,\frac{\hat{\Xi}_{\mathrm{I}}^2\hat{\Xi}_{\mathrm{II}}}{4}\right)-\frac{\hat{\Xi}_{\mathrm{I}}\sqrt{\hat{\Xi}_{\mathrm{II}}}}{2}\mathcal{G}_{0,3}^{3,0}\left(-\flat-\tfrac{1}{2},0,\tfrac{1}{2}\,\middle|\,\frac{\hat{\Xi}_{\mathrm{I}}^2\hat{\Xi}_{\mathrm{II}}}{4}\right)\right)+\frac{(2\flat)!}{\hat{\Xi}_{\mathrm{I}}^{2\flat}} \tag{15}$$

For $p^{(u)}\to+\infty$ (no constraint on the maximum transmit power), $K=0$ (Rayleigh SI channel), $\psi=1$ (compensation factor), and $\beta=4$ (path-loss exponent), we can obtain (15), as shown at the top of this page.

For $p_0\to+\infty$ (no path-loss compensation) and $p^{(u)}\to+\infty$ (no constraint on the maximum transmit power),

$$\mathbb{E}\left\{{p_{k,l}^{(u)}}^{\flat}\right\}=(1+K)^{\flat}\hat{\Xi}_{\mathrm{II}}^{\flat}\Gamma(1-\flat)\,{}_1F_1(\flat;1;-K). \tag{16}$$

Further, for $K=0$ (Rayleigh SI channel),

$$\mathbb{E}\left\{{p_{k,l}^{(u)}}^{\flat}\right\}=\hat{\Xi}_{\mathrm{II}}^{\flat}\Gamma(1-\flat). \tag{17}$$

For $p^{(u)}\to+\infty$) (no constraint on the maximum transmit power) and $I_{SI}\to+\infty$ (no constraint on the SI),

$$\mathbb{E}\left\{{p_{k,l}^{(u)}}^{\flat}\right\}=\frac{\Gamma\left(\frac{\psi\beta\flat}{2}+1\right)}{\hat{\Xi}_{\mathrm{I}}^{\frac{\psi\beta\flat}{2}}}. \tag{18}$$

Further, for $\psi=1$ (compensation factor), and $\beta=4$ (path-loss exponent),

$$\mathbb{E}\left\{{p_{k,l}^{(u)}}^{\flat}\right\}=\frac{\Gamma\left(1+2\flat\right)}{\hat{\Xi}_{\mathrm{I}}^{2\flat}}. \tag{19}$$

Proof: See Appendix C.

IV. Spectral Efficiency Analysis

The notion of doubling the SE by going from HD to FD has been a key driving force behind the surge of interest in this topic. This is however only a theoretical upper-bound concerning point-to-point links under perfect SI cancellation capability. In multi-cell environments, many factors come into play, such as increased interference complexity and intensity, which requires rigorous investigation prior to the potential adoption of FD technology in 5G and beyond.

To facilitate performance analysis and optimization, we provide a framework for the computation of the DL and UL SEs in the massive MIMO-enabled FD cellular network. We utilize a m.g.f.-based methodology, which avoids the need for the direct computation of the SINR p.d.f. by requiring only the m.g.f.s of the different signals involved [45], [46].

A. Downlink Spectral Efficiency

We proceed by providing an explicit expression for the calculation of the SE in the DL.

Theorem 1. *The DL SE in the FD massive MIMO cellular network is given by (20), as shown at the top of the next page.*

Proof: The result follows directly from [45, Lemma 1].

This article has been accepted for publication in a future issue of this journal, but has not been fully edited. Content may change prior to final publication. Citation information: DOI 10.1109/TCOMM.2017.2731768, IEEE Transactions on Communications

$$\mathcal{S}_{d,f} = \mathbb{E}\left\{\log_2\left(1+\gamma_d\right)\right\} = \log_2(e)\int_0^{+\infty}\int_0^{+\infty}\mathcal{M}_{\mathcal{I}_{si,d}|p}(z)\mathcal{M}_{\mathcal{I}_{u,d}|p}(z)\int_0^{+\infty}\left(1-\mathcal{M}_{\mathcal{X}_d|r}(z)\right) \times \mathcal{M}_{\mathcal{I}_{d,d}|r}(z)\frac{\exp\left(-z\sigma_d^2\right)}{z}\mathcal{P}_{p_{k,l}^{(u)}}(p)\,\mathcal{P}_{d_{b,o}}(r)\,\mathrm{d}z\,\mathrm{d}r\,\mathrm{d}p \tag{20}$$

$$\mathcal{M}_{\mathcal{I}_{d,d}|r}(z) = \exp\left(-\pi\lambda^{(d)}\left[r^2\left(\left(z\frac{p^{(d)}}{\mathcal{U}}r^{-\beta}+1\right)^{-\mathcal{U}}-1\right)+\Gamma\left(\mathcal{U}+\frac{2}{\beta}\right)\left(z\frac{p^{(d)}}{\mathcal{U}}\right)^{-\mathcal{U}} \times\left(\left(z\frac{p^{(d)}}{\mathcal{U}}\right)^{\mathcal{U}+\frac{2}{\beta}}\frac{\Gamma\left(1-\frac{2}{\beta}\right)}{\Gamma\left(\mathcal{U}\right)}-\mathcal{U}r^{\mathcal{U}\beta+2}\,{}_2\tilde{F}_1\left(\mathcal{U}+1,\mathcal{U}+\frac{2}{\beta};\mathcal{U}+\frac{2}{\beta}+1;-\frac{r^\beta}{z\frac{p^{(d)}}{\mathcal{U}}}\right)\right)\right]\right) \tag{22}$$

$$\mathcal{M}_{\mathcal{I}_{u,d}|p}(z) = \exp\left(-\pi\mathcal{U}\lambda^{(d)}\left(zp\right)^{\frac{2}{\beta}}\Gamma\left(1-\frac{2}{\beta}\right)\Gamma\left(1+\frac{2}{\beta}\right)\right) \tag{23}$$

$$\mathcal{S}_{u,f} = \mathbb{E}\left\{\log_2\left(1+\gamma_u\right)\right\} = \log_2(e)\int_0^{+\infty}\mathcal{M}_{\mathcal{I}_{d,u}}(z)\int_0^{+\infty}\int_0^{+\infty}\left(1-\mathcal{M}_{\mathcal{X}_u|p,r}(z)\right)\mathcal{M}_{\mathcal{I}_{u,u}|p,r}(z) \times\frac{\exp\left(-z\sigma_u^2\right)}{z}\mathcal{P}_{p_{k,l}^{(u)}}(p)\,\mathcal{P}_{d_{b,o}}(r)\,\mathrm{d}z\,\mathrm{d}r\,\mathrm{d}p \tag{25}$$

$$\mathcal{M}_{\mathcal{I}_{u,u}|p,r}(z) = \exp\left(-\pi\mathcal{U}\lambda^{(d)}\left[\left(zp\right)^{\frac{2}{\beta}}\Gamma\left(1-\frac{2}{\beta}\right)\Gamma\left(1+\frac{2}{\beta}\right)-r^2\left(1-\frac{2r^\beta}{zp\left(\beta+2\right)}\,{}_2F_1\left(1,1+\frac{2}{\beta};2+\frac{2}{\beta};-\frac{r^\beta}{zp}\right)\right)\right]\right) \tag{27}$$

$$\mathcal{M}_{\mathcal{I}_{d,u}}(z) = \exp\left(-\pi\lambda^{(d)}\left(z\frac{p^{(d)}}{\mathcal{U}}\right)^{\frac{2}{\beta}}\frac{\Gamma\left(1-\frac{2}{\beta}\right)\Gamma\left(\mathcal{U}+\frac{2}{\beta}\right)}{\mathcal{U}^{\frac{2}{\beta}}\Gamma\left(\mathcal{U}\right)}\right) \tag{28}$$

Next, we provide explicit expressions for the conditional m.g.f.s of the different DL intended and interfering signals.

Lemma 3. *The conditional m.g.f.s of the different DL signals in the FD massive MIMO cellular network are given by*

$$\mathcal{M}_{\mathcal{X}_d|r}(z) = \left(1+z\frac{p^{(d)}}{\mathcal{U}}r^{-\beta}\right)^{-D_d}, \tag{21}$$

(22), (23), as shown at the top of this page, and

$$\mathcal{M}_{\mathcal{I}_{si,d}|p}(z) = \frac{1+K}{1+K+zp\Omega}\exp\left(-\frac{zpK\Omega}{1+K+zp\Omega}\right). \tag{24}$$

Proof: See Appendix D.

Remark 4. *The CI at the reference MT in (23), is from the aggregation of interference from all other scheduled MTs which are approximated using an independent PPP with spatial density $\mathcal{U}\lambda^{(d)}$ based on Assumption 1.*

B. Uplink Spectral Efficiency

Similarly, we provide a systematic approach for the calculation of the SE in the UL.

Theorem 2. *The UL SE in the FD massive MIMO cellular network is given by (25), as shown at the top of this page.*

Proof: The result follows directly from [45, Lemma 1].

The conditional m.g.f.s of the different UL intended and interfering signals required for SE calculation can be derived in closed-form as in the following lemma.

Lemma 4. *The conditional m.g.f.s of the different UL signals in the FD massive MIMO cellular network are given by*

$$\mathcal{M}_{\mathcal{X}_u|p,r}(z) = \left(1+zpr^{-\beta}\right)^{-D_u}, \tag{26}$$

(27), and (28), as shown at the top of this page.

Proof: See Appendix D.

Remark 5. *The UL inter-cell interference in (27) is derived using a spatially-thinned PPP with spatial density $\mathcal{U}\lambda^{(d)}$ and circular exclusion region with radius r based on the spatial constraints from Assumption 1 [36], [38].*

This article has been accepted for publication in a future issue of this journal, but has not been fully edited. Content may change prior to final publication. Citation information: DOI 10.1109/TCOMM.2017.2731768, IEEE Transactions on Communications

C. Special Cases

In certain special cases, the conditional m.g.f.s of the signals can be simplified further as highlighted in what follows.

Corollary 4. *The conditional m.g.f. of the inter-cell interference in the DL for $\mathcal{U}=1$ (single-user), and $\beta=4$ (path-loss exponent) is given by*

$$\mathcal{M}_{\mathcal{I}_{d,d}|r}(z)=\exp\left(-\pi\lambda^{(d)}\sqrt{zp^{(d)}}\operatorname{arccot}\left(\frac{r^2}{\sqrt{zp^{(d)}}}\right)\right). \tag{29}$$

Corollary 5. *The conditional m.g.f. of the CI in the DL with $\beta=4$ (path-loss exponent) is given by*

$$\mathcal{M}_{\mathcal{I}_{u,d}|p}(z)=\exp\left(-\frac{\pi^2}{2}\mathcal{U}\lambda^{(d)}\sqrt{zp}\right). \tag{30}$$

The above can be further simplified under special cases of UL power control.

For $p^{(u)}\to+\infty$ (no constraint on the maximum transmit power), $K=0$ (Rayleigh SI channel), $\psi=1$ (compensation factor), and $\beta=4$ (path-loss exponent), we can obtain (31), as shown at the bottom of this page.

Further, for $p_0\to+\infty$ (no path-loss compensation),

$$\mathcal{M}_{\mathcal{I}_{u,d}}(z)=\frac{1}{\sqrt{\pi}}\mathcal{G}_{0,3}^{3,0}\left(\left.{}_{0,\frac{1}{2},1}\right|z\hat{\Xi}_{\mathrm{II}}\left(\frac{\pi^2\mathcal{U}\lambda^{(d)}}{4}\right)^2\right). \tag{32}$$

On the other hand, for $I_{SI}\to+\infty$ (no constraint on the SI),

$$\mathcal{M}_{\mathcal{I}_{u,d}}(z)=\frac{1}{1+\frac{\pi}{2}\sqrt{zp_0}}. \tag{33}$$

Corollary 6. *The conditional m.g.f. of the inter-cell interference in the UL for $\beta=4$ (path-loss exponent) is given by*

$$\mathcal{M}_{\mathcal{I}_{u,u}|p,r}(z)=\exp\left(-\pi\mathcal{U}\lambda^{(d)}\sqrt{zp}\operatorname{arccot}\left(\frac{r^2}{\sqrt{zp}}\right)\right). \tag{34}$$

Corollary 7. *The CI conditional m.g.f. in the UL for $\mathcal{U}=1$ (single-user) and $\beta=4$ (path-loss exponent) is given by*

$$\mathcal{M}_{\mathcal{I}_{d,u}}(z)=\exp\left(-\frac{\pi^2}{2}\lambda^{(d)}\sqrt{zp^{(d)}}\right). \tag{35}$$

The SEs in (20) and (25) require three-fold integral computations - versus the manifold integrals involved in the direct p.d.f.-based approach. It is possible to further reduce the computational complexity in certain special cases with UL power control. Note that in the case of baseline SISO, we take into account the SI at the FD BS side.

Lemma 5. *For $N_t,N_r,\mathcal{U}=1$ (baseline SISO), $K=0$ (Rayleigh SI channel), $\sigma_d^2,\sigma_u^2=0$ (interference-limited region), and $\beta=4$ (path-loss exponent), the SEs ($\omega=\frac{p^{(d)}}{p}$ for DL and $\omega=\frac{p}{p^{(d)}}$ for UL) are reduced to double-integral expressions in (36), as shown at the bottom of this page. Further, for SI $=0$ (perfect SI subtraction), the SEs ($\omega=\frac{p^{(d)}}{p}$ for DL and $\omega=\frac{p}{p^{(d)}}$ for UL) are given by (37), as shown at the bottom of this page.*

For $p_0\to+\infty$ (no path-loss compensation) and $p^{(u)}\to+\infty$ (no constraint on the maximum transmit power), the SE expressions in (37) can be reduced to single-fold integrals in (38) and (39), as shown at at the top of the next page.

For $I_{SI}\to+\infty$ (no constraint on the SI) and $p^{(u)}\to+\infty$ (no constraint on the maximum transmit power), the SE expressions in (37) can be reduced to single-fold integrals in (40) and (41), as shown at the top of the next page.

Proof: See Appendix E.

$$\mathcal{M}_{\mathcal{I}_{u,d}}(z)=\frac{1}{1+\frac{\pi}{2}\sqrt{zp_0}}+\frac{1}{\sqrt{\pi}}\mathcal{G}_{0,3}^{3,0}\left(\left.{}_{0,\frac{1}{2},1}\right|\hat{\Xi}_{\mathrm{II}}\left(\frac{\mathcal{U}\hat{\Xi}_{\mathrm{I}}}{2}\left(1+\frac{\pi}{2}\sqrt{zp_0}\right)\right)^2\right)$$
$$-\frac{\mathcal{U}\tilde{\Xi}_{\mathrm{I}}\sqrt{\tilde{\Xi}_{\mathrm{II}}}}{2\sqrt{\pi}}\mathcal{G}_{0,3}^{3,0}\left(\left.{}_{-\frac{1}{2},0,\frac{1}{2}}\right|\hat{\Xi}_{\mathrm{II}}\left(\frac{\mathcal{U}\hat{\Xi}_{\mathrm{I}}}{2}\left(1+\frac{\pi}{2}\sqrt{zp_0}\right)\right)^2\right) \tag{31}$$

$$\mathcal{S}_{\{.\},f}=\log_2(e)\int_0^{+\infty}\int_0^{+\infty}\frac{2\pi\lambda^{(d)}}{\sqrt{\Omega}\left(1+s^2\right)}\sqrt{\omega}\left[\sin\left(\frac{\pi\lambda^{(d)}}{\sqrt{\Omega}}\left(\frac{\pi}{2}+\sqrt{\omega}\left(s+\operatorname{arccot}(s)\right)\right)\right)\right.$$
$$\times\mathscr{C}\left(\frac{\pi\lambda^{(d)}}{\sqrt{\Omega}}\left(\frac{\pi}{2}+\sqrt{\omega}\left(s+\operatorname{arccot}(s)\right)\right)\right)+\cos\left(\frac{\pi\lambda^{(d)}}{\sqrt{\Omega}}\left(\frac{\pi}{2}+\sqrt{\omega}\left(s+\operatorname{arccot}(s)\right)\right)\right)$$
$$\left.\times\left(\frac{\pi}{2}-\mathscr{S}\left(\frac{\pi\lambda^{(d)}}{\sqrt{\Omega}}\left(\frac{\pi}{2}+\sqrt{\omega}\left(s+\operatorname{arccot}(s)\right)\right)\right)\right)\right]\mathcal{P}_{p_{k,l}^{(u)}}(p)\,\mathrm{d}s\,\mathrm{d}p \tag{36}$$

$$\mathcal{S}_{\{.\},f}=\log_2(e)\int_0^{+\infty}\int_0^{+\infty}\frac{2}{\left(1+s^2\right)\left(\frac{\pi}{2\sqrt{\omega}}+s+\operatorname{arccot}(s)\right)}\mathcal{P}_{p_{k,l}^{(u)}}(p)\,\mathrm{d}s\,\mathrm{d}p \tag{37}$$

This article has been accepted for publication in a future issue of this journal, but has not been fully edited. Content may change prior to final publication. Citation information: DOI 10.1109/TCOMM.2017.2731768, IEEE Transactions on Communications

$$\mathcal{S}_{d,f} = \log_2(e) \int_0^{+\infty} \frac{2}{(1+s^2)\left(s+\operatorname{arccot}(s)\right)} \Bigg[1 - \frac{\pi\sqrt{\pi}}{2\left(s+\operatorname{arccot}(s)\right)} \sqrt{\frac{I_{\mathrm{SI}}}{p^{(d)}\Omega}} - \left(\frac{\pi}{2\left(s+\operatorname{arccot}(s)\right)}\right)^2 \frac{I_{\mathrm{SI}}}{p^{(d)}\Omega} \exp\left(-\left(\frac{\pi}{2\left(s+\operatorname{arccot}(s)\right)}\right)^2 \frac{I_{\mathrm{SI}}}{p^{(d)}\Omega}\right) \times \left(\mathrm{Ei}\left(\left(\frac{\pi}{2\left(s+\operatorname{arccot}(s)\right)}\right)^2 \frac{I_{\mathrm{SI}}}{p^{(d)}\Omega}\right) - \pi \mathrm{erfi}\left(\frac{\pi}{2\left(s+\operatorname{arccot}(s)\right)} \sqrt{\frac{I_{\mathrm{SI}}}{p^{(d)}\Omega}}\right)\right)\Bigg] \mathrm{d}s \quad (38)$$

$$\mathcal{S}_{u,f} = \log_2(e) \int_0^{+\infty} \frac{4}{\pi\left(1+s^2\right)} \sqrt{\frac{I_{\mathrm{SI}}}{p^{(d)}\Omega}} \Bigg[\sqrt{\pi} + \frac{2\left(s+\operatorname{arccot}(s)\right)}{\pi} \sqrt{\frac{I_{\mathrm{SI}}}{p^{(d)}\Omega}} \exp\Bigg(-\left(\frac{2\left(s+\operatorname{arccot}(s)\right)}{\pi}\right)^2 \times \frac{I_{\mathrm{SI}}}{p^{(d)}\Omega}\Bigg) \left(\mathrm{Ei}\left(\left(\frac{2\left(s+\operatorname{arccot}(s)\right)}{\pi}\right)^2 \frac{I_{\mathrm{SI}}}{p^{(d)}\Omega}\right) - \pi \mathrm{erfi}\left(\frac{2\left(s+\operatorname{arccot}(s)\right)}{\pi} \sqrt{\frac{I_{\mathrm{SI}}}{p^{(d)}\Omega}}\right)\right)\Bigg] \mathrm{d}s \quad (39)$$

$$\mathcal{S}_{d,f} = \log_2(e) \int_0^{+\infty} \frac{-4\lambda^{(d)}}{1+s^2} \sqrt{\frac{p^{(d)}}{p_0}} \exp\left(2\lambda^{(d)}\left(s+\operatorname{arccot}(s)\right)\sqrt{\frac{p^{(d)}}{p_0}}\right) \mathrm{Ei}\left(-2\lambda^{(d)}\left(s+\operatorname{arccot}(s)\right)\sqrt{\frac{p^{(d)}}{p_0}}\right) \mathrm{d}s \quad (40)$$

$$\mathcal{S}_{u,f} = \log_2(e) \int_0^{+\infty} \frac{2}{\left(1+s^2\right)\left(s+\operatorname{arccot}(s)\right)} \Bigg[1 + \frac{\pi^2\lambda^{(d)}}{2\left(s+\operatorname{arccot}(s)\right)} \sqrt{\frac{p^{(d)}}{p_0}} \times \exp\left(\frac{\pi^2\lambda^{(d)}}{2\left(s+\operatorname{arccot}(s)\right)}\sqrt{\frac{p^{(d)}}{p_0}}\right) \mathrm{Ei}\left(-\frac{\pi^2\lambda^{(d)}}{2\left(s+\operatorname{arccot}(s)\right)}\sqrt{\frac{p^{(d)}}{p_0}}\right)\Bigg] \mathrm{d}s \quad (41)$$

V. Full-Duplex versus Half-Duplex

The SE expressions developed facilitate performance analysis and optimization for generalized FD cellular deployments. At the same time, the proposed framework can serve as a benchmark tool for comparing the performance of FD over HD systems. Although an explicit expression for the corresponding gain cannot be obtained due to the highly complex SE expressions involving multiple improper integrals, we proceed by providing results in certain special cases.

In what follows, $\mathcal{S}_{d,h}$ and $\mathcal{S}_{u,h}$ are respectively used to denote the per-user SEs in the DL and the UL of a HD cellular network. To facilitate performance comparison between the FD and HD systems, we consider the SE over two time slots, i.e., $\mathbb{S}_f = 2(\mathcal{S}_{d,f} + \mathcal{S}_{u,f})$ for FD, and $\mathbb{S}_h = \mathcal{S}_{d,h} + \mathcal{S}_{u,h}$ for HD, respectively. We first study the baseline SISO case and then derive results for the multi-user massive MIMO setup. Network design insights are accordingly drawn.

A. Baseline SISO

Here, we compare the FD versus HD performance for the baseline SISO case.

Lemma 6. *The FD and HD SEs for $N^t, N^r, \mathcal{U} = 1$ (baseline SISO), $p^{(u)}$ (fixed MT transmit power), SI $= 0$ (perfect SI subtraction), $\sigma_d^2, \sigma_u^2 = 0$ (interference-limited region), and $\beta = 4$ (path-loss exponent) are respectively given by (42) and (43), as shown at the bottom of this page. Further, bounded closed-form expressions of the FD and HD SEs are respectively given by (44) and (45), where (46), as shown at the top of the next page.*

Proof: See Appendix F.

$$\mathbb{S}_f = \log_2(e) \int_0^{+\infty} \frac{\frac{2\pi}{1+s^2}\left(\sqrt{\frac{p^{(u)}}{p^{(d)}}} + \sqrt{\frac{p^{(d)}}{p^{(u)}}}\right) + 8\left(s+\operatorname{arccot}(s)\right)}{\left(\frac{\pi}{2}\sqrt{\frac{p^{(u)}}{p^{(d)}}} + s + \operatorname{arccot}(s)\right)\left(\frac{\pi}{2}\sqrt{\frac{p^{(d)}}{p^{(u)}}} + s + \operatorname{arccot}(s)\right)} \mathrm{d}s \quad (42)$$

$$\mathbb{S}_h = \log_2(e) \int_0^{+\infty} \frac{4}{\left(1+s^2\right)\left(s+\operatorname{arccot}(s)\right)} \mathrm{d}s \quad (43)$$

This article has been accepted for publication in a future issue of this journal, but has not been fully edited. Content may change prior to final publication. Citation information: DOI 10.1109/TCOMM.2017.2731768, IEEE Transactions on Communications

$$\tilde{\mathbb{S}}_f \leq 2\log_2(e)\left(\Psi\left(\frac{8}{\pi\left(1+\sqrt{\frac{p^{(u)}}{p^{(d)}}}\right)}-1\right)+\Psi\left(\frac{8}{\pi\left(1+\sqrt{\frac{p^{(d)}}{p^{(u)}}}\right)}-1\right)\right),\ \left(\frac{\pi}{\pi-8}\right)^2<\frac{p^{(d)}}{p^{(u)}}<\left(\frac{\pi-8}{\pi}\right)^2 \tag{44}$$

$$\tilde{\mathbb{S}}_h \leq 2\log_2(e)\Psi\left(\frac{8}{\pi}-1\right) \tag{45}$$

$$\Psi(\alpha)=\frac{(1+\alpha)\left((5-\alpha)\operatorname{arccot}(\sqrt{\alpha})+\sqrt{\alpha}\log\left(\frac{1}{4}(1+\alpha)\right)\right)-\frac{\pi}{2}(5-4\sqrt{\alpha}+\alpha)(1-2\sqrt{\alpha}-\alpha)}{\frac{\sqrt{\alpha}}{1+\alpha}(25-6\alpha+\alpha^2)} \tag{46}$$

$$\underset{x=\frac{p^{(d)}}{p^{(u)}}}{\text{maximize}}\quad \frac{\tilde{\mathbb{S}}_f}{\tilde{\mathbb{S}}_h}=\frac{\Psi\left(\frac{8}{\pi\left(1+\sqrt{x}\right)}-1\right)+\Psi\left(\frac{8}{\pi\left(1+\frac{1}{\sqrt{x}}\right)}-1\right)}{\Psi\left(\frac{8}{\pi}-1\right)}\quad \text{subject to:}\quad \left(\frac{\pi}{\pi-8}\right)^2<x<\left(\frac{\pi-8}{\pi}\right)^2 \tag{47}$$

$$\mathbb{S}_f=\log_2(e)\int_0^{+\infty}\frac{8}{(1+s^2)\left(s+\operatorname{arccot}(s)+\frac{\pi}{2}\right)}\,\mathrm{d}s \tag{49}$$

Remark 6. *The HD SE for the special case described in Lemma 6 is independent of the system parameters. The exact and bounded HD baseline SISO SEs over two time slots (in nat/s/Hz) are approximately* 3 *and* 2.72*, respectively. On the other hand, the exact and bounded FD baseline SISO SEs for this special case are functions of the BS and MT transmit powers only.*

Based on the above remark, we next study the problem of finding the optimal fixed transmit powers which result in the largest FD over HD SE gain for the case of baseline SISO. The SE function in HD mode, $\mathbb{S}_h$ in (43), is affine in $p^{(d)}>0$ and $p^{(u)}>0$. On the other hand, it can be shown that the SE function in FD mode, $\mathbb{S}_f$ in (42), is strictly quasi-concave in $p^{(d)}>0$ and $p^{(u)}>0$. This guarantees the existence of a unique maximum solution under a positive transmit power region. $\mathbb{S}_h$ and $\mathbb{S}_f$, however, involve improper integrals. Thus, an exact closed-form solution cannot be obtained here. Hence, we utilize the bounded SE expressions developed in (44) and (45).

Lemma 7. *Consider the bounded FD and HD SEs for $N^t, N^r, \mathcal{U}=1$ (baseline SISO), $p^{(u)}$ (MT transmit power), SI $=0$ (perfect SI subtraction), $\sigma_d^2, \sigma_u^2=0$ (interference-limited region), and $\beta=4$ (path-loss exponent) from Lemma 6. We can formulate the optimization problem in (47), as shown at the top of this page, for the highest FD over HD SE gain. The solution to this problem is $x^*=1$, resulting in*

$$\left(\frac{\tilde{\mathbb{S}}_f}{\tilde{\mathbb{S}}_h}\right)^*=\frac{2\Psi\left(\frac{4}{\pi}-1\right)}{\Psi\left(\frac{8}{\pi}-1\right)}. \tag{48}$$

Proof: See Appendix G.

Note that with equivalent DL and UL transmit powers, the FD baseline SISO exact SE expression from (42) reduces to (49), as shown at the top of this page.

Remark 7. *Base on the result from Lemma 7, the highest exact and bounded SE percentage gains of FD over HD for baseline SISO are respectively ∼9% and ∼13% (these values also correspond to the individual SE gains in the DL and the UL). We can infer that without advanced techniques for tackling the CI, even under perfect SI subtraction, the FD baseline SISO system achieves only modest improvements in SE over its HD counterpart.*

B. Massive MIMO

Next, we analyze the FD versus HD SE for massive MIMO-enabled cellular networks.

Lemma 8. *The FD and HD SEs with massive MIMO, ZF beamforming, $\mathcal{U}p$ (BS transmit power), p (MT transmit power), SI $=0$ (perfect SI subtraction), $\sigma_d^2, \sigma_u^2=0$ (interference-limited region), and $\beta=4$ (path-loss exponent) are respectively given by (50) and (51), as shown at the top of the next page. For $\mathcal{U}=1$ (single-user), these expressions can be respectively reduced to (52) and (53), as shown at the top of the next page.*

Proof: The proof follows from a similar approach to that provided in Appendix F.

The SE expressions for the case of multi-user massive MIMO derived in Lemma 8 involve single-fold integrals. Next, we employ multivariate non-linear curve fitting in order to provide a closed-form approximation for the FD versus HD massive MIMO SE gain as a function of the number of antennas and users.

This article has been accepted for publication in a future issue of this journal, but has not been fully edited. Content may change prior to final publication. Citation information: DOI 10.1109/TCOMM.2017.2731768, IEEE Transactions on Communications

$$\mathbb{S}_f = \log_2(e)\int_0^{+\infty} \frac{4}{1+s^2}\left(\frac{1+s^2\left(1-\left(1+\frac{1}{s^2}\right)^{\mathcal{U}-N_r}\right)}{s+\mathcal{U}\,\mathrm{arccot}(s)+\sqrt{\frac{\pi}{\mathcal{U}}}\frac{\Gamma\left(\mathcal{U}+\frac{1}{2}\right)}{\Gamma(\mathcal{U})}} + \frac{1+s^2\left(1-\left(1+\frac{1}{s^2}\right)^{\mathcal{U}-N_t}\right)}{\frac{s}{\mathcal{U}}\left(1+\frac{1}{s^2}\right)^{-\mathcal{U}}-s^{2\mathcal{U}+1}\Gamma\left(\mathcal{U}+\frac{1}{2}\right)\,{}_2\tilde{F}_1\left(\mathcal{U}+\frac{1}{2},\mathcal{U}+1;\mathcal{U}+\frac{3}{2};-s^2\right)+\sqrt{\pi}\frac{\Gamma\left(\mathcal{U}+\frac{1}{2}\right)}{\mathcal{U}\Gamma(\mathcal{U})}+\frac{\pi}{2}}\right)\mathrm{d}s \quad (50)$$

$$\mathbb{S}_h = \log_2(e)\int_0^{+\infty} \frac{2}{1+s^2}\left(\frac{1+s^2\left(1-\left(1+\frac{1}{s^2}\right)^{\mathcal{U}-N_r}\right)}{s+\mathcal{U}\,\mathrm{arccot}(s)} + \frac{1+s^2\left(1-\left(1+\frac{1}{s^2}\right)^{\mathcal{U}-N_t}\right)}{s\left(1+\frac{1}{s^2}\right)^{-\mathcal{U}}-\mathcal{U}s^{2\mathcal{U}+1}\Gamma\left(\mathcal{U}+\frac{1}{2}\right)\,{}_2\tilde{F}_1\left(\mathcal{U}+\frac{1}{2},\mathcal{U}+1;\mathcal{U}+\frac{3}{2};-s^2\right)+\sqrt{\pi}\frac{\Gamma\left(\mathcal{U}+\frac{1}{2}\right)}{\Gamma(\mathcal{U})}}\right)\mathrm{d}s \quad (51)$$

$$\mathbb{S}_f = \log_2(e)\int_0^{+\infty} \frac{4}{s+\mathrm{arccot}(s)+\frac{\pi}{2}}\left(2-\left(1+\frac{1}{s^2}\right)^{-N_r}-\left(1+\frac{1}{s^2}\right)^{-N_t}\right)\mathrm{d}s \quad (52)$$

$$\mathbb{S}_h = \log_2(e)\int_0^{+\infty} \frac{2}{s+\mathrm{arccot}(s)}\left(2-\left(1+\frac{1}{s^2}\right)^{-N_r}-\left(1+\frac{1}{s^2}\right)^{-N_t}\right)\mathrm{d}s \quad (53)$$

Corollary 8. *The FD over HD massive MIMO SE gain with ZF beamforming, $\mathcal{N}$ (number of transmit and receive antennas), $\mathcal{U}p$ (BS transmit power), p (MT transmit power), SI $=0$ (perfect SI subtraction), $\sigma_d^2,\sigma_u^2=0$ (interference-limited region), and $\beta=4$ (path-loss exponent) can be approximated using multivariate non-linear curve fitting as*[1]

$$\frac{\mathbb{S}_f}{\mathbb{S}_h} \approx 2-\frac{9}{10}\left(\frac{\mathcal{U}^{\frac{4}{25}}}{\mathcal{N}^{\frac{1}{10}}}\right). \quad (54)$$

Remark 8. *The FD over HD massive MIMO SE gain logarithmically (i) increases in the number of antennas, and (ii) decreases in the number of users. Furthermore, the anticipated two-fold increase in SE of massive MIMO-enabled FD versus HD cellular networks is only achieved as the number of antennas tends to be infinitely large with orders of magnitude smaller number of users ($\mathcal{N}\to+\infty$, $\mathcal{N}\gg\mathcal{U}$).*

It is important to note that the choice of FD over HD operation is primarily to enhance SE, which inherently results in reduced EE [47]. Some potential solutions for alleviating this issue include modified scheduling and power control mechanisms [48]. A rigorous assessment of the EE in FD massive MIMO cellular networks is postponed to future work.

VI. Numerical Results

In this section, we provide several numerical examples in order to assess the performance of the FD massive MIMO cellular network under different settings of system parameters. MC simulations are accordingly provided for the purpose of examining the validity of the proposed analytical framework. The BS deployment density is considered to be $\lambda^{(d)}=\frac{4}{\pi}$ per unit area (km×km). The total system bandwidth is taken to be $B=20$ MHz. The noise powers in the DL and the UL are calculated using $\sigma^2=-170+10\log_{10}(B)+N_f$ (dBm), where N_f is the noise figure [49]. Note that the results from the MC simulations are obtained considering (i) the scheduled MTs follow from a PPP (*Assumption 1*), (ii) non-central Chi-squared distribution for the SI channel power gains (*Assumption 3*), and (iii) Gamma distribution for the other channels power gains (*Assumptions 2 and 4*).

1) Different FD Cellular Setups: We compare the DL and UL SE performance of different FD cellular networks, namely, massive MIMO (with ZF-SIN precoder and ZF decoder) and baseline SISO in Fig. 1. In order to facilitate a fair comparison whilst capturing the inherent characteristics of the two systems, we consider (i) per-user SEs, although each massive MIMO BS is considered to be serving several MTs per resource block, (ii) greater BS transmit power in the baseline SISO case, and (iii) equivalent residual SI channel statistics. The results confirm prior findings that the UL rate is the main performance bottleneck in FD cellular systems with baseline SISO. Here, the UL performance is severely limited due to the impact of CI, especially with the large disparity in the BS and MT transmit power levels, as well as the imperfect SI subtraction. Furthermore, it can be observed that significant SE gains in the DL and (especially) in the UL can be achieved by exploiting the large scale antenna array with linear ZF-SIN precoding and linear ZF decoding. By increasing the antenna array size, further improvements can be realized from (i) greater transmit/receive antenna array gains, and (ii) the

[1]The properties related to the goodness of fit of the closed-form approximation in (54) are $R^2\approx 0.999$ and estimated variance of $\approx 1.17\times10^{-3}$.

This article has been accepted for publication in a future issue of this journal, but has not been fully edited. Content may change prior to final publication. Citation information: DOI 10.1109/TCOMM.2017.2731768, IEEE Transactions on Communications

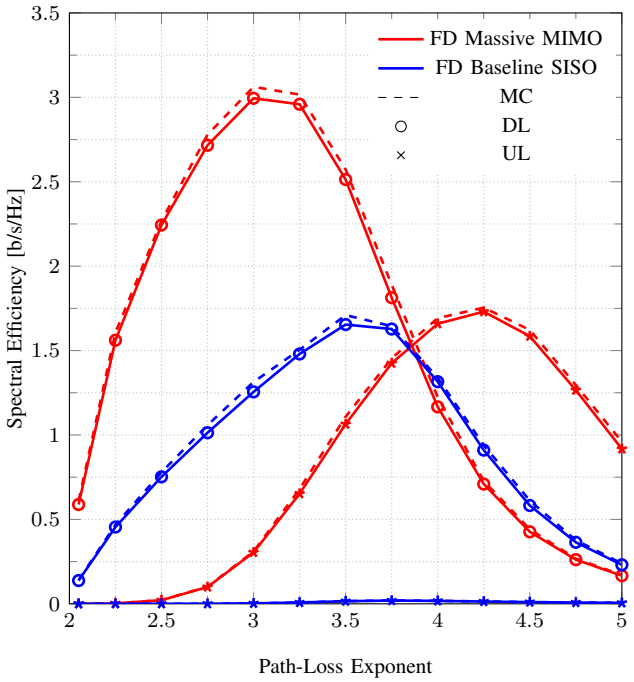

Fig. 1. System parameters are: $\lambda^{(d)} = \frac{4}{\pi}$ BSs/km^2, massive MIMO ($N_t = 80$, $N_r = 20$, $\mathcal{U} = 8$, $p^{(d)} = 30$ dBm), baseline SISO ($N_t = 1$, $N_r = 1$, $\mathcal{U} = 1$, $p^{(d)} = 43$ dBm), $p^{(u)} = 23$ dBm, $p_0 = -80$ dBm, $B = 20$ MHz, $N_f = 10$ dB, $\psi = 1$, $\Omega = -80$ dB, $K = 1$.

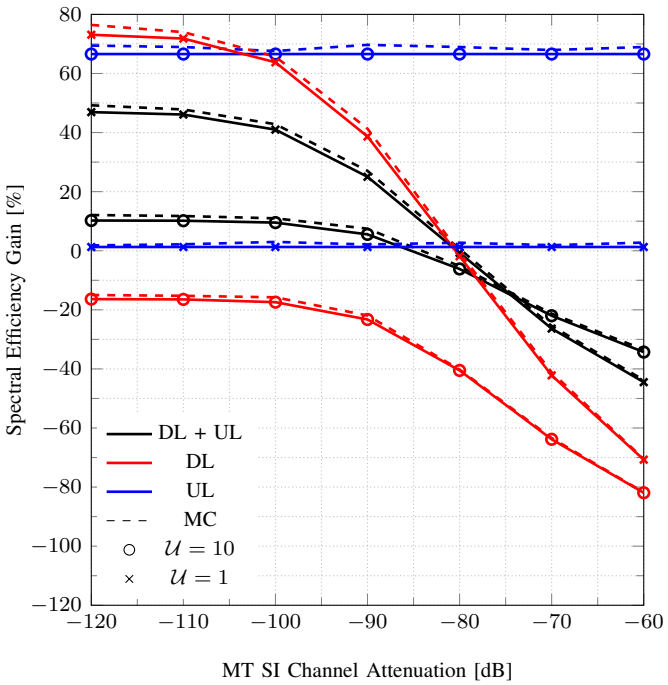

Fig. 2. System parameters are: $\lambda^{(d)} = \frac{4}{\pi}$ BSs/km^2, $N_t = 350$, $N_r = 50$, $p^{(d)} = 30$ dBm, $p^{(u)} = 23$ dBm, $p_0 = -80$ dBm, $B = 20$ MHz, $N_f = 10$ dB, $\beta = 4$, $\psi = 1$, $K = 1$.

potential to linearly reduce the transmit powers of the BSs and MTs without degrading the received signal-to-noise ratio (SNR). It should be noted that the MC results confirm the validity of the proposed analytical framework.

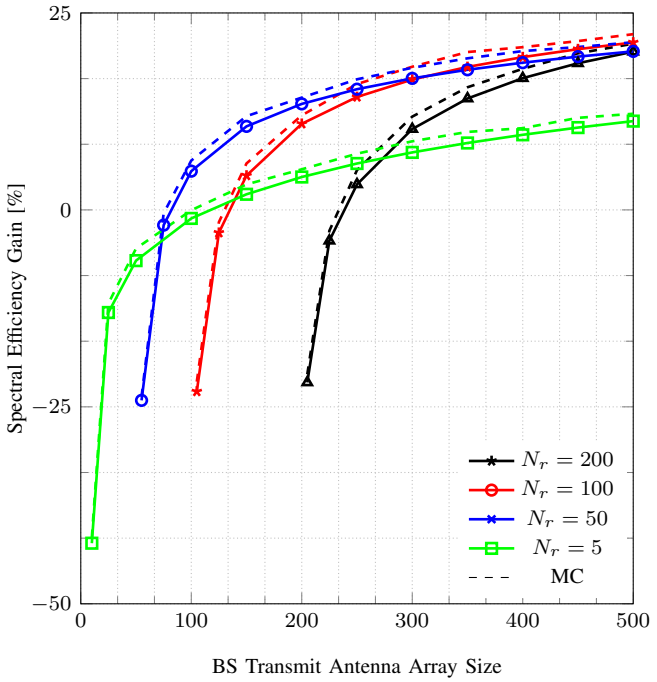

Fig. 3. System parameters are: $\lambda^{(d)} = \frac{4}{\pi}$ BSs/km^2, $\mathcal{U} = 5$, $p^{(d)} = 30$ dBm, $p^{(u)} = 23$ dBm, $p_0 = -80$ dBm, $B = 20$ MHz, $N_f = 10$ dB, $\beta = 4$, $\psi = 1$, $\Omega = -90$ dB, $K = 2$.

2) FD versus HD Massive MIMO: Next, we investigate the performance of the FD massive MIMO cellular network with respect to its HD counterpart over a wide range of MT SI channel attenuation in Fig. 2. It can be seen that any potential improvements from the FD operation occurs for MT SI channel attenuation well below -80 dB. This trend indicates that unless advanced interference mitigation solutions are available at the MTs, the FD technology should be strictly used at the BS side (serving HD DL and UL MTs). Nevertheless, even with nearly perfect SI cancellation capability at the reference FD MT, with single-user MIMO ($\mathcal{U} = 1$), the maximum SE gain of the FD massive MIMO cellular network over its analogous HD variant is 47% (resulting from 73% and 1% increases in the DL and UL SEs, respectively). It should be noted that this negligible change in the UL SE comes as a result of the overwhelming CI from the BSs transmitting in the DL in FD mode. In addition, it can be seen from Fig. 2 that by increasing the number of MTs (whilst using the same total transmit power at the BS side), the FD over HD UL SE gain may be improved, however, this comes at the cost of reduced relative DL SE gain due to the additional CI from the MTs transmitting in the UL in FD mode.

3) Transmit/Receive Antenna Array Size: The impact of the different number of transmit and receive antennas on the SE gain of the massive MIMO-enabled FD system over its HD counterpart is illustrated in Fig. 3. It can be observed that the corresponding performance gain increases in the number of transmit antennas due to the reduced impact of the DL array gain loss from the ZF-SIN precoding scheme and improved resilience against interference. The optimal ratio of transmit over receive antennas, on the other hand, depends on the

This article has been accepted for publication in a future issue of this journal, but has not been fully edited. Content may change prior to final publication. Citation information: DOI 10.1109/TCOMM.2017.2731768, IEEE Transactions on Communications

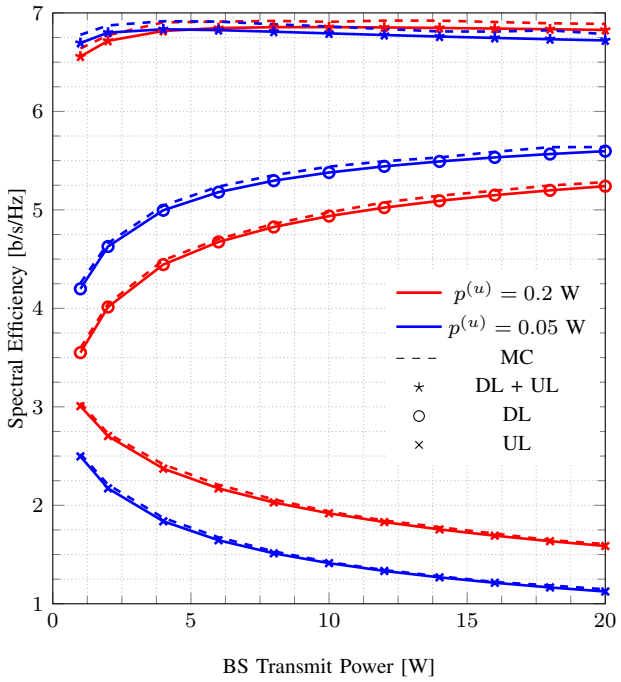

Fig. 4. System parameters are: $\lambda^{(d)} = \frac{4}{\pi}$ BSs/km^2, $N_t = 150$, $N_r = 50$, $\mathcal{U} = 4$, $p_0 = -80$ dBm, $B = 20$ MHz, $N_f = 10$ dB, $\beta = 4$, $\psi = 1$, $\Omega = -100$ dB, $K = 0$.

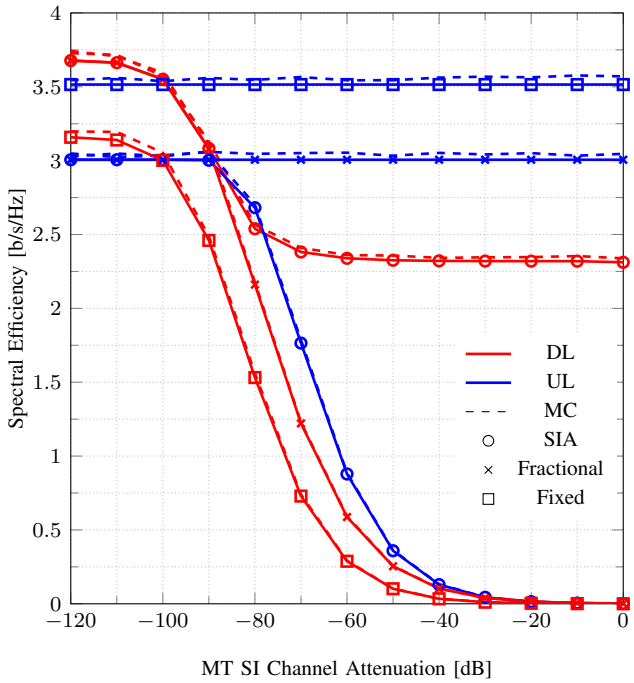

Fig. 5. System parameters are: $\lambda^{(d)} = \frac{4}{\pi}$ BSs/km^2, $N_t = 150$, $N_r = 50$, $\mathcal{U} = 4$, $p^{(d)} = 30$ dBm, $p^{(u)} = 23$ dBm, $p_0 = -80$ dBm, $\frac{I_{\text{SI}}}{\sigma^2} = 25$ dB, $p_f^{(u)} = 23$ dBm, $B = 20$ MHz, $N_f = 10$ dB, $\beta = 4$, $\psi = 1$, $K = 0$.

particular system settings. A rigorous study of this aspect is left to future work. It is important to note that the results from Fig. 3 reaffirm our theoretical findings in Remark 8, that the FD over HD massive MIMO SE gain increases only logarithmically in the antenna array size.

4) Transmit Power Budget: It has been shown in [4] that the transmit energy can be linearly conserved in the number of antennas. This is a contributing factor in tackling the FD UL rate bottleneck through massive MIMO, as was demonstrated in Fig. 1. We depict the impact of different BS transmit power and MT maximum transmit power in Fig. 4. Intuitively, increasing $p^{(d)}$, or $p^{(u)}$, respectively improves the corresponding SE in the DL, or the UL; the relative gain however decreases for larger power budgets. Further, the DL and UL SEs are conflicting functions in the BS/MT transit powers. In general, we observe that a large difference in the DL/UL power levels is deteriorating to the overall performance in FD mode. Due to the large disparity in the DL/MT SEs, however, the direct optimization of the FD sum-rate places the focus on the DL, see Fig. 4. It is therefore important for any respective optimization to strike a balance (e.g., by applying weights) between the DL and UL SEs. This is however beyond the scope of this work.

5) Uplink Power Control: The results presented so far were based on the conventional UL fractional power control mechanism defined in the existing LTE standards for HD cases. Next, we study the performance of the massive MIMO-enabled FD cellular network with different fixed (at maximum power), conventional, and proposed SIA fractional power control protocols under different SI channel attenuation in Fig. 5. It can be observed that the lack of self-interference-awareness in the case of fixed as well as fractional power allocation strategies means that the DL performance significantly suffers in the case of large MT SI channel attenuation. The proposed scheme can therefore serve as an important safe-guard mechanism for ensuring that a certain maximum SI level is not exceeded.

VII. Summary

We provided a theoretical framework using tools from stochastic geometry and point processes for the study of massive MIMO-enabled FD cellular networks. The DL and UL SEs with linear ZF-SIN precoding, SIA fractional power control, and linear ZF receiver were characterized over Rician SI and Rayleigh intended and other-interference fading channels. The results highlighted the promising potential of massive MIMO towards unlocking the UL rate bottleneck in FD communication systems. On the other hand, the results demonstrated that the anticipated two-fold increase in SE of the massive MIMO-enabled FD cellular network overs its HD variant is only achievable in the asymptotic antenna region.

Appendix A

To jointly suppress the (residual) SI and multi-user interference in the DL, considering $\boldsymbol{G}_l$, $\boldsymbol{H}_l$, and $\boldsymbol{G}_{l,l}$ are full-rank and estimated without error, the conditions (i) $\boldsymbol{W}_l\boldsymbol{G}_{l,l}\boldsymbol{V}_l = \boldsymbol{0}_{\mathcal{U}\times\mathcal{U}}$, and (ii) $\boldsymbol{g}_{l,k}\boldsymbol{v}_{l,j} = 0$, $\forall j \neq k$ must be satisfied. The singular value decomposition (SVD) of $\boldsymbol{G}_{l,l}$ is given by $\mathbb{U}_{l,l}\boldsymbol{\Sigma}_{l,l}\left[\mathbb{V}_{l,l}^{(1)}\mathbb{V}_{l,l}^{(0)}\right]^{\dagger}$ where $\mathbb{U}_{l,l}$ holds the left singular vectors, $\boldsymbol{\Sigma}_{l,l}$ is the matrix of singular values, and $\mathbb{V}_{l,l}^{(1)}$ and $\mathbb{V}_{l,l}^{(0)}$ are the right singular matrices of the non-zero and zero

This article has been accepted for publication in a future issue of this journal, but has not been fully edited. Content may change prior to final publication. Citation information: DOI 10.1109/TCOMM.2017.2731768, IEEE Transactions on Communications

singular values, respectively [50]. For SI nulling, the precoder is designed such that its column vectors are in the nullspace of $\boldsymbol{G}_{l,l}$ (i.e., $\boldsymbol{V}_l = \mathbb{V}_{l,l}^{(0)}$) using $\mathbf{I}_{N_t} - \boldsymbol{G}_{l,l}^{\dagger}(\boldsymbol{G}_{l,l}\boldsymbol{G}_{l,l}^{\dagger})^{-1}\boldsymbol{G}_{l,l}$. At the same time, to suppress multi-user interference in the DL, we design the proposed ZF-SIN precoder $\boldsymbol{V}_l$ using the pseudo-inverse of the projection channel matrix $\hat{\boldsymbol{G}}_l = \boldsymbol{G}_l(\mathbf{I}_{N_t} - \boldsymbol{G}_{l,l}^{\dagger}(\boldsymbol{G}_{l,l}\boldsymbol{G}_{l,l}^{\dagger})^{-1}\boldsymbol{G}_{l,l})$. ■

APPENDIX B

The proposed SIA fractional power control mechanism c.d.f. can be expressed as

$$\mathcal{F}_{p_{k,l}^{(u)}}(p) = \left(1 - \mathcal{H}\left(p - p^{(u)}\right)\right) \times \mathscr{P}\left(\hat{p}_k^{(u)} \leq p\right) + \mathcal{H}\left(p - p^{(u)}\right) \quad \text{(B.1)}$$

where $\hat{p}_k^{(u)} = \min\left(p_0 d_{k,l}^{\psi\beta}, I_{\text{SI}} H_{k,k}^{-1}\right)$. Hence, we can write

$$\begin{aligned}\mathcal{F}_{\hat{p}_k^{(u)}}(p) &= \mathcal{F}_{p_0 d_{k,l}^{\psi\beta}}(p) + \mathcal{F}_{I_{\text{SI}}H_{k,k}^{-1}}(p) - \mathcal{F}_{p_0 d_{k,l}^{\psi\beta}}(p)\,\mathcal{F}_{I_{\text{SI}}H_{k,k}^{-1}}(p) \\ &= \mathscr{P}\left(d_{k,l} \leq \left(\frac{p}{p_0}\right)^{\frac{1}{\psi\beta}}\right) + \mathscr{P}\left(H_{k,k} \geq \frac{I_{\text{SI}}}{p}\right) \\ &\quad - \mathscr{P}\left(d_{k,l} \leq \left(\frac{p}{p_0}\right)^{\frac{1}{\psi\beta}}\right)\mathscr{P}\left(H_{k,k} \geq \frac{I_{\text{SI}}}{p}\right). \quad \text{(B.2)}\end{aligned}$$

By considering the transmitter-receiver distance distribution,

$$\begin{aligned}&\mathscr{P}\left(d_{k,l} \leq \left(\frac{p}{p_0}\right)^{\frac{1}{\psi\beta}}\right) \\ &= \int_0^{\left(\frac{p}{p_0}\right)^{\frac{1}{\psi\beta}}} 2\pi\lambda^{(d)} r \exp\left(-\pi\lambda^{(d)} r^2\right) \mathrm{d}r \\ &= 1 - \exp\left(-\pi\lambda^{(d)}\left(\frac{p}{p_0}\right)^{\frac{2}{\psi\beta}}\right), \quad \text{(B.3)}\end{aligned}$$

and the SI channel power gain non-central Chi-squared distribution,

$$\begin{aligned}&\mathscr{P}\left(H_{k,k} \geq \frac{I_{\text{SI}}}{p}\right) \\ &= \int_{\frac{I_{\text{SI}}}{p}}^{+\infty} \frac{1+K}{\Omega} \exp\left(-\left(K + \frac{(1+K)h}{\Omega}\right)\right) \\ &\quad \times I_0\left(2\sqrt{\frac{K(1+K)h}{\Omega}}\right) \mathrm{d}h \\ &= Q_1\left(\sqrt{2K}, \sqrt{\frac{2(1+K)I_{\text{SI}}}{p\Omega}}\right), \quad \text{(B.4)}\end{aligned}$$

we can obtain

$$\begin{aligned}\mathcal{F}_{\hat{p}_k^{(u)}}(p) &= 1 - \exp\left(-\pi\lambda^{(d)}\left(\frac{p}{p_0}\right)^{\frac{2}{\psi\beta}}\right) \\ &\quad \left(1 - Q_1\left(\sqrt{2K}, \sqrt{\frac{2(1+K)I_{\text{SI}}}{p\Omega}}\right)\right). \quad \text{(B.5)}\end{aligned}$$

Through differentiating the above, we can derive the p.d.f. expression in (B.6), as shown at the top of the next page. Hence, with some basic algebraic manipulations, we arrive at Lemma 1. ■

APPENDIX C

Consider the case where the p.d.f. of the UL transmit power is given by

$$\begin{aligned}&\mathcal{P}_{p_{k,l}^{(u)}}(p) = \exp\left(-\pi\lambda^{(d)}\sqrt{\frac{p}{p_0}}\right) \\ &\times\left[\frac{2\pi\lambda^{(d)}}{4p}\sqrt{\frac{p}{p_0}}\left(1 - \exp\left(-\frac{I_{\text{SI}}}{p\Omega}\right)\right) + \frac{I_{\text{SI}}}{p^2\Omega}\exp\left(-\frac{I_{\text{SI}}}{p\Omega}\right)\right]. \quad \text{(C.1)}\end{aligned}$$

By utilizing the integral identities (where $n > 0$ and $\flat > n$)

$$\int_0^{+\infty} \exp\left(-x^n\right) x^{\flat - n}\, \mathrm{d}x = \frac{\Gamma\left(\frac{1-n-\flat}{n}\right)}{n} \quad \text{(C.2)}$$

and

$$\int_0^{+\infty} \exp\left(-\sqrt{x} - \frac{1}{x}\right) x^{\flat - n}\, \mathrm{d}x = \frac{\mathcal{G}_{0,3}^{3,0}\left(\begin{matrix} n-\flat-1, 0, \frac{1}{2} \\ \end{matrix}\middle|\, \frac{1}{4}\right)}{\sqrt{\pi}}, \quad \text{(C.3)}$$

we can arrive at (15).

Next, consider the following transmit power p.d.f.

$$\begin{aligned}\mathcal{P}_{p_{k,l}^{(u)}}(p) &= \frac{(1+K)I_{\text{SI}}}{p^2\Omega}\exp\left(-\left(K + \frac{(1+K)I_{\text{SI}}}{p\Omega}\right)\right) \\ &\quad \times {}_0\tilde{F}_1\left(;1;\frac{K(1+K)I_{\text{SI}}}{p\Omega}\right). \quad \text{(C.4)}\end{aligned}$$

We derive the following integral identity (where $\flat < 1$ and $n > \flat$)

$$\begin{aligned}&\int_0^{+\infty} \exp\left(\frac{1}{p}\right) {}_0\tilde{F}_1\left(;1;\frac{1}{p}\right) p^{\flat - n}\, \mathrm{d}p \\ &= L_{\flat - n + 1}(1)\Gamma(n - \flat - 1). \quad \text{(C.5)}\end{aligned}$$

Hence, by utilizing $\mathcal{L}_m(z) = {}_0\tilde{F}_1(-m;1;z)$, we can arrive at (16). It should be noted that with no path-loss compensation, the first and beyond positive moments ($\flat \geq 1$) of $p_{k,l}^{(u)}$ are infinite.

Finally, note the following unbounded transmit power p.d.f.

$$\mathcal{P}_{p_{k,l}^{(u)}}(p) = \frac{2\pi\lambda^{(d)}}{\psi\beta p}\left(\frac{p}{p_0}\right)^{\frac{2}{\psi\beta}} \exp\left(-\pi\lambda^{(d)}\left(\frac{p}{p_0}\right)^{\frac{2}{\psi\beta}}\right). \quad \text{(C.6)}$$

By utilizing the integral identity (C.2), we can obtain (18). ■

APPENDIX D

Let Φ, λ, and $\mathscr{E}$ denote the PPP, density, and exclusion region radius, respectively. Hence, $\mathcal{I} = \sum_{x\in\Phi} Q_x \|x\|^{-\beta}$ where x and Q_x are respectably the location and channel power gain of an arbitrary interferer with respect to a typical receiver at the origin. We proceed as follows

$$\mathcal{M}_{\mathcal{I}}(z) = \mathbb{E}\left\{\exp\left(-z\sum_{x\in\Phi} Q_x \|x\|^{-\beta}\right)\right\}$$

This article has been accepted for publication in a future issue of this journal, but has not been fully edited. Content may change prior to final publication. Citation information: DOI 10.1109/TCOMM.2017.2731768, IEEE Transactions on Communications

$$\mathcal{P}_{\hat{p}_k^{(u)}}(p)=\exp\left(-\pi\lambda^{(d)}\left(\frac{p}{p_0}\right)^{\frac{2}{\psi\beta}}\right)\left(\frac{2\pi\lambda^{(d)}}{\psi\beta p}\left(\frac{p}{p_0}\right)^{\frac{2}{\beta\psi}}\left(1-Q_1\left(\sqrt{2K},\sqrt{\frac{2(K+1)I_{\mathrm{SI}}}{p\Omega}}\right)\right)\right.$$
$$\left.+\frac{(1+K)I_{\mathrm{SI}}}{p^2\Omega}\exp\left(-\left(K+\frac{(1+K)I_{\mathrm{SI}}}{p\Omega}\right)\right){}_0\tilde{F}_1\left(;1;\frac{K(1+K)I_{\mathrm{SI}}}{p\Omega}\right)\right) \quad \text{(B.6)}$$

$$\stackrel{(i)}{=}\lim_{\mathscr{D}\to+\infty}\mathbb{E}_{\mathscr{N}}\left\{\left(\mathbb{E}_{Q_x,x}\left\{\exp\left(-zQ_x\|x\|^{-\beta}\right)\right\}\right)^{\mathscr{N}}\right\}$$
$$\stackrel{(ii)}{=}\lim_{\mathscr{D}\to+\infty}\exp\left(\pi\lambda\left(\mathscr{D}^2-\mathscr{E}^2\right)\times\left(\mathbb{E}_{Q_x,x}\left\{\exp\left(-zQ_x\|x\|^{-\beta}\right)\right\}-1\right)\right)$$
$$\stackrel{(iii)}{=}\lim_{\mathscr{D}\to+\infty}\exp\left(2\pi\lambda\mathbb{E}_{Q_x}\left(\int_{\mathscr{E}}^{\mathscr{D}}\mathcal{R}\times\left(\exp\left(-zQ_x\|\mathcal{R}\|^{-\beta}-1\right)\right)\mathrm{d}\mathcal{R}\right)\right)$$
$$\stackrel{(iv)}{=}\exp\left(-\pi\lambda\mathbb{E}_{Q_x}\left\{\left[\Gamma\left(1-\frac{2}{\beta}\right)-\Gamma\left(1-\frac{2}{\beta},zQ_x\mathscr{E}^{-\beta}\right)\right]\times\left(zQ_x\right)^{\frac{2}{\beta}}+\mathscr{E}^2\left(\exp\left(-zQ_x\mathscr{E}^{-\beta}\right)-1\right)\right\}\right) \quad \text{(D.1)}$$

where (i) is written considering $\mathscr{N}$ conditional interferers are i.i.d. in a circular region of radius $\mathscr{D}$ $(>\mathscr{E})$ around the center with the limit as $\mathscr{D}\to+\infty$; (ii) is from characterizing $\mathscr{N}$ as a Poisson random variable with expected value $\pi\lambda\left(\mathscr{D}^2-\mathscr{E}^2\right)$ and hence utilizing the Poisson identity $\mathbb{E}\left\{\zeta^{\mathscr{N}}\right\}=\exp\left(\mathbb{E}\left\{\mathscr{N}\right\}(\zeta-1)\right)$; (iii) is written using the p.d.f. of the distance $\mathcal{R}$ (where $\mathscr{E}<\mathcal{R}<\mathscr{D}$)

$$\mathcal{P}_{\|x\|}(\mathcal{R})=\frac{2\mathcal{R}}{\mathscr{D}^2-\mathscr{E}^2}; \quad \text{(D.2)}$$

(iv) is obtained by invoking the integral identity (where $\alpha>0$ and $\beta>2$)

$$\mathbb{E}_{\|x\|}\left\{\exp\left(-\alpha\|x\|^{-\beta}\right)\right\}=\frac{2\alpha^{\frac{2}{\beta}}}{\beta\left(\mathscr{D}^2-\mathscr{E}^2\right)}\times\left[\Gamma\left(-\frac{2}{\beta},\frac{\alpha}{\mathscr{D}^\beta}\right)-\Gamma\left(-\frac{2}{\beta},\frac{\alpha}{\mathscr{E}^\beta}\right)\right], \quad \text{(D.3)}$$

and taking the limit as $\mathscr{D}\to+\infty$.

To proceed, the distribution of the channel power gain should be specified. Here, we consider the general case where $Q_x\sim\Gamma(U,V)$, which can be used to capture a wide range of MIMO setups [46]. Hence, through utilizing the following integral identities (where $\alpha>0$ and $\beta>2$)

$$\mathbb{E}_{Q_x}\left\{Q_x^{\frac{2}{\beta}}\right\}=\frac{\Gamma\left(U+\frac{2}{\beta}\right)}{\Gamma(U)}V^{\frac{2}{\beta}}, \quad \text{(D.4)}$$

$$\mathbb{E}_{Q_x}\left\{\Gamma\left(1-\frac{2}{\beta},\alpha Q_x\right)\right\}=\frac{\Gamma\left(U-\frac{2}{\beta}+1\right)}{(\alpha V)^U\Gamma(U+1)}\times{}_2F_1\left(U,U-\frac{2}{\beta}+1;U+1;-\frac{1}{\alpha V}\right), \quad \text{(D.5)}$$

and

$$\mathbb{E}_{Q_x}\left\{\exp\left(-\alpha Q_x\right)\right\}=\frac{1}{(1+\alpha V)^U}, \quad \text{(D.6)}$$

we can arrive at

$$\mathcal{M}_{\mathcal{I}}(z)=\exp\left(-\pi\lambda\left[-\mathscr{E}^2+\frac{\mathscr{E}^2}{\left(zV\mathscr{E}^{-\beta}+1\right)^U}+\frac{\Gamma\left(1-\frac{2}{\beta}\right)\Gamma\left(U+\frac{2}{\beta}\right)}{\Gamma(U)}(zV)^{\frac{2}{\beta}}-\frac{U\beta}{U\beta+2}\frac{\mathscr{E}^{U\beta+2}}{(zV)^U}\right.\right.$$
$$\left.\left.\times{}_2F_1\left(U+1,U+\frac{2}{\beta};U+\frac{2}{\beta}+1;-\frac{\mathscr{E}^\beta}{zV}\right)\right]\right). \quad \text{(D.7)}$$

■

APPENDIX E

Consider the cases where the DL and UL SEs are respectively simplified to

$$\mathcal{S}_{d,f}=\log_2(e)\int_0^{+\infty}\int_0^{+\infty}\int_0^{+\infty}\frac{2\pi\lambda^{(d)}rp^{(d)}}{(1+zp\Omega)\left(r^4+zp^{(d)}\right)}\exp\left(-\pi\lambda^{(d)}\left(\frac{\pi}{2}\sqrt{zp}+\sqrt{zp^{(d)}}\arctan\left(\frac{\sqrt{zp^{(d)}}}{r^2}\right)+r^2\right)\right)\mathcal{P}_{p_{k,l}^{(u)}}(p)\,\mathrm{d}z\,\mathrm{d}r\,\mathrm{d}p \quad \text{(E.1)}$$

and

$$\mathcal{S}_{u,f}=\log_2(e)\int_0^{+\infty}\int_0^{+\infty}\int_0^{+\infty}\frac{2\pi\lambda^{(d)}rp}{1+zp^{(d)}\Omega)\left(r^4+zp\right)}\exp\left(-\pi\lambda^{(d)}\left(\frac{\pi}{2}\sqrt{zp^{(d)}}+\sqrt{zp}\arctan\left(\frac{\sqrt{zp}}{r^2}\right)+r^2\right)\right)\mathcal{P}_{p_{k,l}^{(u)}}(p)\,\mathrm{d}z\,\mathrm{d}r\,\mathrm{d}p. \quad \text{(E.2)}$$

Utilizing, in the order given, substitution with $\frac{z}{p^{(d)}}\to u^4$, conversion from Cartesian to polar coordinates with $u\to\mathscr{R}\sin(\mathscr{T})$ and $r\to\mathscr{R}\cos(\mathscr{T})$ (with Jacobian $\mathscr{R}$), the integral identity

$$\int_0^{+\infty}\frac{\mathscr{R}}{1+\mathscr{R}^4}\exp\left(-\mathscr{R}^2\right)\mathrm{d}\mathscr{R}=\frac{1}{2}\left(\sin(1)\mathscr{C}(1)+\left(\frac{\pi}{2}-\cos(1)\mathscr{S}(1)\right)\right), \quad \text{(E.3)}$$

and substitution with $\mathscr{T}\to\arctan\sqrt{s}$, we can arrive at (36). The same process can be applied in the case of complete SI removal but with the reduced integral identity (C.1) to obtain

This article has been accepted for publication in a future issue of this journal, but has not been fully edited. Content may change prior to final publication. Citation information: DOI 10.1109/TCOMM.2017.2731768, IEEE Transactions on Communications

(37). Finally, we can respectively arrive at (38)-(39) using

$$\int_0^{+\infty} \frac{1}{p\left(p+\sqrt{p}\right)} \exp\left(-\frac{1}{p}\right) \mathrm{d}p = \sqrt{\pi} + \frac{1}{e}\mathrm{Ei}(1) - \frac{\pi}{e}\mathrm{erfi}(1) \tag{E.4}$$

and at (40)-(41) using

$$\int_0^{+\infty} \frac{1}{p+\sqrt{p}} \exp\left(-\sqrt{p}\right)\, dp = -2\exp(1)\mathrm{Ei}(-1). \tag{E.5}$$

■

APPENDIX F

By computing the special case of $2\left(\mathcal{S}_{d,f}+\mathcal{S}_{u,f}\right)$ and $\left(\mathcal{S}_{d,h}+\mathcal{S}_{u,h}\right)$ using the approach in Appendix E, we can readily obtain (42) and (43), respectively.

Utilizing the approximation (where $s \geq 0$)

$$\arctan(s) = \arcsin\left(\sqrt{\frac{s^2}{1+s^2}}\right) \geq \frac{s}{1+s}, \tag{F.1}$$

the integral identity (where $\alpha > \frac{1}{4}$)

$$\begin{aligned}\int_0^{\infty} &\frac{1+s}{\left(1+s^2\right)\left(\alpha s^2+s+1\right)}\ \mathrm{d}s \\ &= \frac{1}{\sqrt{4\alpha-1}\left(\alpha^2-2\alpha+2\right)} \\ &\times\Bigg(\pi\left(\alpha^2-\frac{\alpha}{2}\left(\sqrt{4\alpha-1}+3\right)+\sqrt{4\alpha-1}\right) \\ &+\frac{\alpha}{2}\sqrt{4\alpha-1}\log(\alpha)-\alpha(2\alpha-3)\,\mathrm{arccot}\left(\sqrt{4\alpha-1}\right)\Bigg),\end{aligned} \tag{F.2}$$

and basic algebraic manipulation, we derive (44) and (45). ■

APPENDIX G

We proceed by defining the super-level set of $\frac{\mathbb{S}_f}{\mathbb{S}_h}$ in x as

$$\mathcal{L} = \left\{ x \in \mathbf{dom}\ \frac{\mathbb{S}_f}{\mathbb{S}_h} \middle| \frac{\mathbb{S}_f}{\mathbb{S}_h} \geq \mathscr{K} \right\}. \tag{G.1}$$

For the case in which $\mathscr{K} < 0$, the total SE gain of FD over HD is always positive, hence, there are no points on the counter, $\left(\frac{\mathbb{S}_f}{\mathbb{S}_h}\right)^* = \mathscr{K}$. On the other hand, for $\mathscr{K} > 0$, we can write

$$\begin{aligned}\frac{\mathbb{S}_f}{\mathbb{S}_h} &= \frac{2\left(\mathcal{S}_{d,f}+\mathcal{S}_{u,f}\right)}{\mathcal{S}_{d,h}+\mathcal{S}_{u,h}} \\ &= \frac{\Psi\left(\frac{8}{\pi\left(1+\sqrt{x}\right)}-1\right)+\Psi\left(\frac{8}{\pi\left(1+\frac{1}{\sqrt{x}}\right)}-1\right)}{\Psi\left(\frac{8}{\pi}-1\right)}\end{aligned} \tag{G.2}$$

with

$$\begin{aligned}\mathcal{L} \equiv \Psi\left(\frac{8}{\pi}-1\right)\mathscr{K} - \Bigg(&\Psi\left(\frac{8}{\pi\left(1+\sqrt{x}\right)}-1\right) \\ &+\Psi\left(\frac{8}{\pi\left(1+\frac{1}{\sqrt{x}}\right)}-1\right)\Bigg) \leq 0.\end{aligned} \tag{G.3}$$

The joint HD DL/UL SE in the above is affine in x. It can be shown that the second derivative of the SE function in FD mode, $\frac{\mathrm{d}^2}{\mathrm{d}x^2}\left(2\left(\mathbb{S}_{d,f}+\mathbb{S}_{d,f}\right)\right)$, is always positive for $\left(\frac{\pi}{\pi-8}\right)^2 < x < 1$, always negative for $1 < x < \left(\frac{\pi-8}{\pi}\right)^2$, and zero for $x = 1$. Consequently, $\mathcal{L}$ is convex in x and the objective function in (47) is strictly quasi-concave in x, with a maximum point at $x^* = 1$. ■

REFERENCES

[1] A. Shojaeifard, K. K. Wong, M. D. Renzo, K. A. Hamdi, and J. Tang, "Design and analysis of full-duplex massive MIMO cellular networks," in *Proc. IEEE Globecom (GC) Wkshps.*, Dec. 2016, pp. 1–6.

[2] A. Shojaeifard, K. K. Wong, M. D. Renzo, G. Zheng, K. A. Hamdi, and J. Tang, "Full-duplex versus half-duplex large scale antenna system," in *Proc. IEEE Int. Conf. Commun. (ICC) Wkshps.*, May 2017, pp. 743–748.

[3] F. Boccardi, R. W. Heath, A. Lozano, T. L. Marzetta, and P. Popovski, "Five disruptive technology directions for 5G," *IEEE Commun. Mag.*, vol. 52, no. 2, pp. 74–80, Feb. 2014.

[4] H. Q. Ngo, E. G. Larsson, and T. L. Marzetta, "Energy and spectral efficiency of very large multiuser MIMO systems," *IEEE Trans. Commun.*, vol. 61, no. 4, pp. 1436–1449, Apr. 2013.

[5] M. Duarte, C. Dick, and A. Sabharwal, "Experiment-driven characterization of full-duplex wireless systems," *IEEE Trans. Wireless Commun.*, vol. 11, no. 12, pp. 4296–4307, Dec. 2012.

[6] E. Everett, A. Sahai, and A. Sabharwal, "Passive self-interference suppression for full-duplex infrastructure nodes," *IEEE Trans. Wireless Commun.*, vol. 13, no. 2, pp. 680–694, Feb. 2014.

[7] M. Chung, M. S. Sim, J. Kim, D. K. Kim, and C. B. Chae, "Prototyping real-time full duplex radios," *IEEE Commun. Mag.*, vol. 53, no. 9, pp. 56–63, Sept. 2015.

[8] D. Kim, H. Lee, and D. Hong, "A survey of in-band full-duplex transmission: From the perspective of PHY and MAC layers," *IEEE Commun. Surveys Tuts.*, vol. 17, no. 4, pp. 2017–2046, Fourth Quart. 2015.

[9] D. Nguyen, L. N. Tran, P. Pirinen, and M. Latva-aho, "On the spectral efficiency of full-duplex small cell wireless systems," *IEEE Trans. Wireless Commun.*, vol. 13, no. 9, pp. 4896–4910, Sept. 2014.

[10] I. Atzeni and M. Kountouris, "Full-duplex MIMO small-cell networks: Performance analysis," *arXiv:1504.04167*, 2015.

[11] S. Goyal, C. Galiotto, N. Marchetti, and S. Panwar, "Throughput and coverage for a mixed full and half duplex small cell network," *arXiv:1602.09115*, 2016.

[12] G. Zhang, K. Yang, P. Liu, and J. Wei, "Power allocation for full-duplex relaying-based D2D communication underlaying cellular networks," *IEEE Trans. Veh. Technol.*, vol. 64, no. 10, pp. 4911–4916, Oct. 2015.

[13] N. Pappas, M. Kountouris, A. Ephremides, and A. Traganitis, "Relay-assisted multiple access with full-duplex multi-packet reception," *IEEE Trans. Wireless Commun.*, vol. 14, no. 7, pp. 3544–3558, July 2015.

[14] M. Mohammadi, B. K. Chalise, H. A. Suraweera, C. Zhong, G. Zheng, and I. Krikidis, "Throughput analysis and optimization of wireless-powered multiple antenna full-duplex relay systems," *IEEE Trans. Commun.*, vol. 64, no. 4, pp. 1769–1785, Apr. 2016.

[15] M. Mohammadi, H. A. Suraweera, and C. Tellambura, "Full-duplex cloud-RAN with uplink/downlink remote radio head association," *arXiv:1602.08836*, 2016.

[16] A. AlAmmouri, H. ElSawy, O. Amin, and M. Alouini, "In-band full-duplex communications for cellular networks with partial uplink/downlink overlap," *arXiv:1508.02909*, 2015.

[17] A. Sadeghi, M. Luvisotto, F. Lahouti, S. Vitturi, and M. Zorzi, "Statistical QoS analysis of full duplex and half duplex heterogeneous cellular networks," *arXiv:1604.00588*, 2016.

[18] L. Wang, F. Tian, T. Svensson, D. Feng, M. Song, and S. Li, "Exploiting full duplex for device-to-device communications in heterogeneous networks," *IEEE Commun. Mag.*, vol. 53, no. 5, pp. 146–152, May 2015.

[19] A. AlAmmouri, H. ElSawy, and M. S. Alouini, "Flexible design for α-duplex communications in multi-tier cellular networks," *IEEE Trans. Commun.*, vol. 64, no. 8, pp. 3548–3562, Aug. 2016.

[20] A. Sabharwal, P. Schniter, D. Guo, D. W. Bliss, S. Rangarajan, and R. Wichman, "In-band full-duplex wireless: Challenges and opportunities," *IEEE J. Sel. Areas Commun.*, vol. 32, no. 9, pp. 1637–1652, Sept. 2014.

[21] G. Y. Li, M. Bennis, and G. Yu, "Full duplex communications [guest editorial]," *IEEE Commun. Mag.*, vol. 53, no. 5, p. 90, May 2015.

[22] B. Yin, M. Wu, C. Studer, J. R. Cavallaro, and J. Lilleberg, "Full-duplex in large-scale wireless systems," in *Proc. Asilomar Conf. Signals, Syst. and Comput. (ASILOMAR)*, Nov. 2013, pp. 1623–1627.

[23] K. Min, S. Park, Y. Jang, T. Kim, and S. Choi, "Antenna ratio for sum-rate maximization in full-duplex large-array base station with half-duplex multi-antenna users," *IEEE Trans. Veh. Technol.*, accepted 2016.

[24] Y.-G. Lim, D. Hong, and C.-B. Chae, "Performance analysis of self-interference cancellation methods in full-duplex large-scale MIMO systems," *arXiv:1508.02166*, 2015.

[25] S. Huberman and T. Le-Ngoc, "Full-duplex MIMO precoding for sum-rate maximization with sequential convex programming," *IEEE Trans. Veh. Technol.*, vol. 64, no. 11, pp. 5103–5112, Nov. 2015.

[26] J. Kim, W. Choi, and H. Park, "Beamforming for full-duplex multiuser MIMO systems," *IEEE Trans. Veh. Technol.*, accepted 2016.

[27] J. Bai and A. Sabharwal, "Asymptotic analysis of MIMO multi-cell full-duplex networks," *IEEE Trans. Wireless Commun.*, vol. 16, no. 4, pp. 2168–2180, Apr. 2017.

[28] M. A. A. Khojastepour, K. Sundaresan, S. Rangarajan, and M. Farajzadeh-Tehrani, "Scaling wireless full-duplex in multi-cell networks," in *Proc. IEEE Conf. Computer Commun. (INFOCOM)*, April 2015, pp. 1751–1759.

[29] I. Atzeni and M. Kountouris, "Full-duplex MIMO small-cell networks with interference cancellation," *arXiv:1612.07289*, 2016.

[30] C. Psomas, M. Mohammadi, I. Krikidis, and H. A. Suraweera, "Impact of directionality on interference mitigation in full-duplex cellular networks," *IEEE Trans. Wireless Commun.*, vol. 16, no. 1, pp. 487–502, Jan. 2017.

[31] R. Li, Y. Chen, G. Y. Li, and G. Liu, "Full-duplex cellular networks: It works!" *arXiv:1604.02852*, 2016.

[32] L. Wang, K. K. Wong, M. Elkashlan, A. Nallanathan, and S. Lambotharan, "Secrecy and energy efficiency in massive MIMO aided heterogeneous C-RAN: A new look at interference," *IEEE J. Sel. Topics Signal Process.*, vol. 10, no. 8, pp. 1375–1389, Dec. 2016.

[33] S. N. Chiu, D. Stoyan, W. S. Kendall, and J. Mecke, *Stochastic geometry and its applications*. John Wiley & Sons, 2013.

[34] A. Shojaeifard, K. A. Hamdi, E. Alsusa, D. K. C. So, and J. Tang, "A unified model for the design and analysis of spatially-correlated load-aware HetNets," *IEEE Trans. Commun.*, vol. 62, no. 11, pp. 1–16, Nov. 2014.

[35] F. Boccardi, J. Andrews, H. Elshaer, M. Dohler, S. Parkvall, P. Popovski, and S. Singh, "Why to decouple the uplink and downlink in cellular networks and how to do it," *IEEE Commun. Mag.*, vol. 54, no. 3, pp. 110–117, Mar. 2016.

[36] M. D. Renzo and P. Guan, "Stochastic geometry modeling and system-level analysis of uplink heterogeneous cellular networks with multi-antenna base stations," *IEEE Trans. Commun.*, vol. 64, no. 6, pp. 2453–2476, June 2016.

[37] E. Björnson, J. Hoydis, M. Kountouris, and M. Debbah, "Massive MIMO systems with non-ideal hardware: Energy efficiency, estimation, and capacity limits," *IEEE Trans. Inf. Theory*, vol. 60, no. 11, pp. 7112–7139, Nov. 2014.

[38] T. Bai and R. W. Heath, "Analyzing uplink SINR and rate in massive MIMO systems using stochastic geometry," *IEEE Trans. Commun.*, vol. 64, no. 11, pp. 4592–4606, Nov. 2016.

[39] A. Shojaeifard, K. A. Hamdi, E. Alsusa, D. K. C. So, J. Tang, and K. K. Wong, "Design, modeling, and performance analysis of multi-antenna heterogeneous cellular networks," *IEEE Trans. Commun.*, vol. 64, no. 7, pp. 3104–3118, July 2016.

[40] A. Shojaeifard, K. K. Wong, M. D. Renzo, G. Zheng, K. A. Hamdi, and J. Tang, "Self-interference in full-duplex multi-user MIMO channels," *IEEE Commun. Lett.*, vol. 21, no. 4, pp. 841–844, Apr. 2017.

[41] S. Parkvall, A. Furuskar, and E. Dahlman, "Evolution of LTE toward IMT-advanced," *IEEE Commun. Mag.*, vol. 49, no. 2, pp. 84–91, Feb. 2011.

[42] F. J. Martin-Vega, G. Gomez, M. C. Aguayo-Torres, and M. D. Renzo, "Analytical modeling of interference aware power control for the uplink of heterogeneous cellular networks," *IEEE Trans. Wireless Commun.*, vol. 15, no. 10, pp. 6742–6757, Oct. 2016.

[43] A. Shojaeifard, K. A. Hamdi, E. Alsusa, D. K. C. So, and J. Tang, "Exact SINR statistics in the presence of heterogeneous interferers," *IEEE Trans. Inform. Theory*, vol. 61, no. 12, pp. 6759–6773, Dec. 2015.

[44] V. Adamchik and O. Marichev, "The algorithm for calculating integrals of hypergeometric type functions and its realization in REDUCE system," in *Proc. Int. Symp. Symbolic and Algebraic Computation*. ACM, 1990.

[45] K. Hamdi, "A useful lemma for capacity analysis of fading interference channels," *IEEE Trans. Commun.*, vol. 58, no. 2, pp. 411–416, Feb. 2010.

[46] M. Di Renzo, A. Guidotti, and G. Corazza, "Average rate of downlink heterogeneous cellular networks over generalized fading channels: A stochastic geometry approach," *IEEE Trans. Commun.*, vol. 61, no. 7, pp. 3050–3071, July 2013.

[47] D. Nguyen, L. N. Tran, P. Pirinen, and M. Latva-aho, "Precoding for full duplex multiuser MIMO systems: Spectral and energy efficiency maximization," *IEEE Trans. Sig. Process.*, vol. 61, no. 16, pp. 4038–4050, Aug. 2013.

[48] S. Goyal, P. Liu, S. S. Panwar, R. A. Difazio, R. Yang, and E. Bala, "Full duplex cellular systems: will doubling interference prevent doubling capacity?" *IEEE Commun. Mag.*, vol. 53, no. 5, pp. 121–127, May 2015.

[49] A. He, L. Wang, M. Elkashlan, Y. Chen, and K. K. Wong, "Spectrum and energy efficiency in massive MIMO enabled HetNets: A stochastic geometry approach," *IEEE Commun. Lett.*, vol. 19, no. 12, pp. 2294–2297, Dec. 2015.

[50] Q. H. Spencer, A. L. Swindlehurst, and M. Haardt, "Zero-forcing methods for downlink spatial multiplexing in multiuser MIMO channels," *IEEE Trans. Signal Process.*, vol. 52, no. 2, pp. 461–471, Feb. 2004.